

Pilot-Aided Distributed Multi-Group Multicast Precoding Design for Cell-Free Massive MIMO

Bikshapathi Gouda, *Student Member, IEEE*, Italo Atzeni, *Member, IEEE*,
and Antti Tölli, *Senior Member, IEEE*

Abstract

We propose fully distributed multi-group multicast precoding designs for cell-free massive multiple-input multiple-output (MIMO) systems with modest training overhead. We target the minimization of the sum of the maximum mean squared errors (MSEs) over the multicast groups, which is then approximated with a weighted sum MSE minimization to simplify the computation and signaling. To design the joint network-wide multi-group multicast precoders at the base stations (BSs) and the combiners at the user equipments (UEs) in a fully distributed fashion, we adopt an iterative bi-directional training scheme with UE-specific or group-specific precoded uplink pilots and group-specific precoded downlink pilots. To this end, we introduce a new group-specific uplink training resource that entirely eliminates the need for backhaul signaling for the channel state information (CSI) exchange. The precoders are optimized locally at each BS by means of either best-response or gradient-based updates, and the convergence of the two approaches is analyzed with respect to the centralized implementation with perfect CSI. Finally, numerical results show that the proposed distributed methods greatly outperform conventional cell-free massive MIMO precoding designs that rely solely on local CSI.

I. INTRODUCTION

Emerging shared wireless applications, such as video streaming, vehicular communications, augmented/mixed reality, and wireless coded caching, considerably increase the demand for multicasting services [2]. The multicast precoding framework was initially developed to transmit a single data stream to a group of user equipments (UEs) [3]. This was subsequently extended in [4] to serve several multicast groups with parallel data streams, each transmitted using a group-specific precoder under a rate constraint imposed by the worst UE in the multicast group. The conventional objective considered for the multi-group multicast precoding design is the max-min fairness (MMF), according to which the minimum signal-to-interference-plus-noise ratio (SINR) in each multicast group is maximized under a transmit power constraint [3], [4]. For this

The authors are with the Centre for Wireless Communications, University of Oulu, Finland. The work of B. Gouda and A. Tölli was supported by the Academy of Finland (318927 6G Flagship). The work of I. Atzeni was supported by the Academy of Finland (348396 HIGH-6G and 336449 Profif6). Part of this work will be presented at IEEE GLOBECOM 2022 [1].

objective, [5], [6] proposed low-complexity methods to design the optimal multi-group multicast precoders. Such precoders have a similar structure to the weighted minimum mean squared error (MMSE) precoder, where the matched filtering (MF) front-end is given by a weighted sum of the effective channels in the multicast group [5].

The aforementioned works assume perfect channel state information (CSI) at the transmitter. However, in practice, the UE-specific channels need to be estimated. In time division duplexing (TDD) systems, this can be done via reverse link measurements, which usually require as many orthogonal pilots as the number of UEs. The number of orthogonal pilots can be substantially reduced by assigning a common pilot to all the UEs in a multicast group [7]. Hence, considering the resulting training overhead, using group-specific rather than UE-specific pilots for the multi-group multicast precoding design has the potential to increase the effective rate. The effective performance of multi-group multicasting in massive multiple-input multiple-output (MIMO) systems was analyzed in [8] under different precoding and pilot assignment strategies. This study was extended in [9] to include coexisting unicast and multi-group multicast transmissions. The multi-group multicast precoding design in a coordinated multi-cell scenario was considered in [10]–[12], where the CSI is assumed to be exchanged among the BSs via backhaul signaling.

Cell-free massive MIMO is an extension of joint transmission coordinated multi-point to a UE-centric approach, where all the BSs jointly serve all the UEs to eliminate the inter-cell interference [2], [13], [14]. To facilitate the UE-centric joint processing, the BSs are connected to a central processing unit (CPU) via backhaul links to exchange the UE-specific data and CSI. Most works on cell-free massive MIMO consider simple local precoding strategies, such as MF, local (regularized) zero forcing, and local MMSE precoding [14]–[16], to circumvent the prohibitive complexity and backhaul signaling of large-scale centralized precoding designs. However, allowing (limited) coordination among the BSs to enable more advanced precoding strategies can provide significant performance gains [16]–[19]. In our previous work [20], we considered a cell-free massive MIMO unicasting scenario and proposed a fully distributed method based on iterative bi-directional training [21] to design the joint network-wide MMSE precoders locally at each BS. This scheme eliminates the need for backhaul signaling for the CSI exchange altogether and yields a performance close to that of the centralized implementation with perfect CSI.

Cell-free massive MIMO is especially suited for multicasting applications as it improves the rate of the cell-edge UEs and thus reduces the impact of the worst UE within each multicast group. Multi-group multicasting in cell-free massive MIMO systems has been considered, for

example, in [22]–[24], where MF precoding is used for the data transmission. Equal power allocation among the multicast precoders at each BS was assumed in [22] to eliminate the need for backhaul signaling for the CSI exchange, whereas the optimal power allocation across the multicast groups was carried out in [23], [24] while assuming limited backhaul signaling.

A. Contribution

Most works on cell-free massive MIMO multi-group multicasting assume MF precoding to avoid the complexity and backhaul signaling issues associated with the centralized precoding design [22]–[24]. In this paper, we propose a distributed framework to design the multi-group multicast precoders with low complexity and without any backhaul signaling for the CSI exchange.

We begin by targeting the minimization of the sum of the maximum mean squared errors (MSEs) over the multicast groups, which is referred to in the following as the *sum-group MSE*. This approach achieves absolute MSE fairness within each multicast group, which is dictated by slowly varying dual variables that would need to be exchanged among the BSs via backhaul signaling in the distributed precoding designs. To avoid the resulting backhaul signaling overhead, we approximate the sum-group MSE minimization with a weighted sum MSE minimization, which greatly simplifies the distributed precoding design while only slightly relaxing the MSE fairness requirement. In this regard, we show that the in-built MSE fairness of the weighted sum MSE metric provides a good approximation for the original sum-group MSE metric, especially at high signal-to-noise ratio (SNR). Based on the reformulated problem, we propose a novel framework to design the joint network-wide multi-group multicast precoders at the BSs and the combiners at the UEs in a fully distributed fashion. To this end, we adopt an iterative bi-directional training mechanism [21] with UE-specific or group-specific precoded uplink pilots and group-specific precoded downlink pilots. The iterative optimization of the precoders is carried out via either best-response or gradient-based updates, and the convergence of the two approaches is analyzed with respect to the centralized implementation with perfect CSI. In our previous works on distributed precoding design for cell-free massive MIMO unicasting [20], [25], we introduced a UE-specific over-the-air (OTA) uplink training resource to facilitate the distributed precoding design. In this paper, we propose a new group-specific OTA uplink training resource tailored for the multi-group multicasting scenario, which entirely eliminates the need for backhaul signaling for the CSI exchange and enables the proposed distributed precoding designs with modest training overhead. Moreover, the proposed framework can straightforwardly handle the coexistence of multicasting

and unicasting by simply considering individual UEs as separate multicast groups. Numerical results show that the proposed distributed methods bring substantial gains over conventional cell-free massive MIMO precoding designs that rely solely on local CSI. Furthermore, the methods based on group-specific pilots always yield the best effective performance.

Part of this work is included in our conference paper [1], which presents the distributed multi-group multicast precoding design with best-response updates. In this paper, we additionally propose an enhanced distributed method with gradient-based updates exploiting group-specific pilots, and prove the asymptotic equivalence of the sum-group MSE and sum MSE objectives. Furthermore, we provide a detailed description of all the proposed schemes and analyze their convergence with respect to the centralized implementation with perfect CSI. Lastly, we present comprehensive numerical results based on a wide range of system parameters.

Outline. The rest of the paper is structured as follows. Section II introduces the system model for cell-free massive MIMO multi-group multicasting along with the iterative bi-directional training and channel estimation. Section III describes the sum-group MSE minimization and the approximation with a weighted sum MSE minimization with reference to the centralized implementation with perfect CSI; moreover, it introduces the reference precoding schemes. The proposed distributed multi-group multicast precoding designs with best-response and gradient-based updates are presented in Sections IV and V for perfect and imperfect CSI, respectively. Finally, Sections VI and VII provide the numerical results and the concluding remarks, respectively.

Notation. Lowercase and uppercase boldface letters denote vectors and matrices, respectively. $(\cdot)^T$ and $(\cdot)^H$ are the transpose and Hermitian transpose operators, respectively. $\|\cdot\|$ and $\|\cdot\|_F$ represent the Euclidean norm for vectors and the Frobenius norm for matrices, respectively. $\text{Re}[\cdot]$ and $\mathbb{E}[\cdot]$ are the real part and expectation operators, respectively. \mathbf{I}_L denotes the L -dimensional identity matrix and $\mathbf{0}$ represents a zero vector with proper dimension. $\text{Diag}(\cdot)$ and $\text{blkdiag}(\cdot)$ represent diagonal and block-diagonal matrices, respectively. $[a_1, \dots, a_L]$ denotes horizontal concatenation, whereas $\{a_1, \dots, a_L\}$ and $\{a_\ell\}_{\ell \in \mathcal{L}}$ represent sets. $\mathcal{CN}(0, \sigma^2)$ is the complex normal distribution with zero mean and variance σ^2 . Lastly, $\nabla_{\mathbf{x}}(\cdot)$ denotes the gradient with respect to \mathbf{x} , whereas $\mathcal{L}_{(a)}(\cdot)$ represents the Lagrangian of optimization problem (a).

II. SYSTEM MODEL

Consider a cell-free massive MIMO system where a set of BSs $\mathcal{B} \triangleq \{1, \dots, B\}$ serves a set of UEs $\mathcal{K} \triangleq \{1, \dots, K\}$ in the downlink. Each BS and UE are equipped with M and N

antennas, respectively. The UEs are divided into a set of non-overlapping multicast groups $\mathcal{G} \triangleq \{1, \dots, G\}$, with \mathcal{K}_g denoting the set of UEs in group $g \in \mathcal{G}$. In the following, we use g_k as the index of the group that contains UE k . The BSs transmit a single data stream to each multicast group, i.e., all the UEs $k \in \mathcal{K}_g$ are intended to receive the same data symbol d_g . Assuming TDD mode, let $\mathbf{H}_{b,k} \in \mathbb{C}^{M \times N}$ be the uplink channel matrix between UE $k \in \mathcal{K}$ and BS $b \in \mathcal{B}$, and let $\mathbf{w}_{b,g} \in \mathbb{C}^{M \times 1}$ be the BS-specific precoder used by BS b for group g . We use $\mathbf{H}_k \triangleq [\mathbf{H}_{1,k}^T, \dots, \mathbf{H}_{B,k}^T]^T \in \mathbb{C}^{BM \times N}$ and $\mathbf{w}_g \triangleq [\mathbf{w}_{1,g}^T, \dots, \mathbf{w}_{B,g}^T]^T \in \mathbb{C}^{BM \times 1}$ to denote the aggregated uplink channel matrix of UE k and the aggregated precoder used for group g , respectively, which imply $\mathbf{H}_k^H \mathbf{w}_g = \sum_{b \in \mathcal{B}} \mathbf{H}_{b,k}^H \mathbf{w}_{b,g}$. We assume the per-BS transmit power constraints $\sum_{g \in \mathcal{G}} \|\mathbf{w}_{b,g}\|^2 \leq \rho_{\text{BS}}, \forall b \in \mathcal{B}$, where ρ_{BS} denotes the maximum transmit power at each BS. Hence, the signal received at UE k is given by

$$\mathbf{y}_k \triangleq \sum_{b \in \mathcal{B}} \mathbf{H}_{b,k}^H \mathbf{w}_{b,g_k} d_{g_k} + \sum_{b \in \mathcal{B}} \sum_{\bar{g} \neq g_k} \mathbf{H}_{b,k}^H \mathbf{w}_{b,\bar{g}} d_{\bar{g}} + \mathbf{z}_k \in \mathbb{C}^{N \times 1}, \quad (1)$$

where $\mathbf{z}_k \in \mathbb{C}^{N \times 1}$ is the additive white Gaussian noise (AWGN) with i.i.d. $\mathcal{CN}(0, \sigma_{\text{UE}}^2)$ elements. Upon receiving \mathbf{y}_k , UE k obtains a soft estimate of d_g by applying the combiner $\mathbf{v}_k \in \mathbb{C}^{N \times 1}$ and the resulting SINR can be expressed as

$$\gamma_k \triangleq \frac{|\sum_{b \in \mathcal{B}} \mathbf{v}_k^H \mathbf{H}_{b,k}^H \mathbf{w}_{b,g_k}|^2}{\sum_{\bar{g} \neq g_k} |\sum_{b \in \mathcal{B}} \mathbf{v}_k^H \mathbf{H}_{b,k}^H \mathbf{w}_{b,\bar{g}}|^2 + \sigma_{\text{UE}}^2 \|\mathbf{v}_k\|^2}. \quad (2)$$

Finally, the sum of the rates over the multicast groups, which is referred to in the following as the *sum-group rate*, is given by $R \triangleq \sum_{g \in \mathcal{G}} R_g$, where R_g is the rate of group g defined as

$$R_g \triangleq \min_{k \in \mathcal{K}_g} \log_2(1 + \gamma_k) \quad [\text{bps/Hz}]. \quad (3)$$

Note that (3) represents an upper bound on the system performance that is attained with perfect global CSI at all the BSs and UEs [26].

In this paper, we aim to design the joint network-wide multi-group multicast precoders at the BSs and the combiners at the UEs in a fully distributed fashion. To this end, we adopt an iterative bi-directional training scheme that relies on estimating the effective uplink and downlink channels via precoded pilots, as discussed in detail in the following section.

A. Iterative Bi-Directional Training and Pilot-Aided Channel Estimation

The centralized precoding design (considered as a reference scheme) involves the transmission of antenna-specific uplink pilots, by which each BS estimates the antenna-specific uplink channels.

Antenna-specific uplink channel estimation (UL). The estimation of the uplink channel $\mathbf{H}_{b,k}$ involves N antenna-specific uplink pilots for UE k . In this context, let $\mathbf{P}_k^{\text{UL}} \in \mathbb{C}^{\tau \times N}$ be the uplink

pilot matrix of UE k , with $\|\mathbf{P}_k^{\text{UL}}\|_{\text{F}}^2 = \tau^{\text{UL}}N$, $\forall k \in \mathcal{K}$. Moreover, let ρ_{UE} denote the maximum transmit power at each UE. Each UE k synchronously transmits its pilot matrix \mathbf{P}_k^{UL} , i.e.,

$$\mathbf{X}_k^{\text{UL}} \triangleq \sqrt{\beta^{\text{UL}}}(\mathbf{P}_k^{\text{UL}})^{\text{H}} \in \mathbb{C}^{N \times \tau^{\text{UL}}}, \quad (4)$$

where the power scaling factor $\beta^{\text{UL}} \triangleq \frac{\rho_{\text{UE}}}{N}$ (equal for all the UEs) ensures that \mathbf{X}_k^{UL} complies with the per-UE transmit power constraint. Then, the signal received at BS b is given by

$$\mathbf{Y}_b^{\text{UL}} \triangleq \sum_{k \in \mathcal{K}} \mathbf{H}_{b,k} \mathbf{X}_k^{\text{UL}} + \mathbf{Z}_b^{\text{UL}} = \sqrt{\beta^{\text{UL}}} \sum_{k \in \mathcal{K}} \mathbf{H}_{b,k} (\mathbf{P}_k^{\text{UL}})^{\text{H}} + \mathbf{Z}_b^{\text{UL}} \in \mathbb{C}^{M \times \tau^{\text{UL}}}, \quad (5)$$

where \mathbf{Z}_b^{UL} is the AWGN with i.i.d. $\mathcal{CN}(0, \sigma_{\text{BS}}^2)$ elements. Finally, the least-squares (LS) estimate of $\mathbf{H}_{b,k}$ is

$$\hat{\mathbf{H}}_{b,k} \triangleq \frac{1}{\tau^{\text{UL}} \sqrt{\beta^{\text{UL}}}} \mathbf{Y}_b^{\text{UL}} \mathbf{P}_k^{\text{UL}} = \mathbf{H}_{b,k} + \frac{1}{\tau^{\text{UL}}} \sum_{\bar{k} \neq k} \mathbf{H}_{b,\bar{k}} (\mathbf{P}_{\bar{k}}^{\text{UL}})^{\text{H}} \mathbf{P}_k^{\text{UL}} + \frac{1}{\tau^{\text{UL}} \sqrt{\beta^{\text{UL}}}} \mathbf{Z}_b^{\text{UL}} \mathbf{P}_k^{\text{UL}} \in \mathbb{C}^{M \times N}, \quad (6)$$

where the last equality holds if $(\mathbf{P}_k^{\text{UL}})^{\text{H}} \mathbf{P}_k^{\text{UL}} = \tau^{\text{UL}} \mathbf{I}_N$, i.e., if there is no pilot contamination among the antennas of UE k .

On the other hand, the proposed distributed precoding designs and the local precoding designs (also considered as reference schemes) are based on *iterative bi-directional training*, whereby the precoders at the BSs and the combiners at the UEs are updated iteratively by means of uplink and downlink pilot-aided channel estimation [19], [21], [27]. Specifically, each bi-directional training iteration involves:

- i)* The transmission of UE-specific or group-specific precoded uplink pilots from all the UEs, by which each BS estimates the UE-specific or group-specific effective uplink channels and updates its precoders;
- ii)* The transmission of precoded downlink pilots from all the BSs, by which each UE estimates its effective downlink channel and updates its combiner.

In the following, we describe the different types of pilot-aided channel estimation that are adopted within the iterative bi-directional training, which will be heavily utilized in Sections III-C and V. In Section V, we further introduce a new group-specific OTA uplink training resource tailored for the multi-group multicasting scenario, which entirely eliminates the need for backhaul signaling for the CSI exchange and enables the proposed distributed precoding designs with modest training overhead.

UE-specific effective uplink channel estimation (UL-1). Let $\mathbf{h}_{b,k} \triangleq \mathbf{H}_{b,k} \mathbf{v}_k \in \mathbb{C}^{M \times 1}$ be the effective uplink channel between UE k and BS b , and let $\mathbf{p}_k^{\text{UL-1}} \in \mathbb{C}^{\tau^{\text{UL-1}} \times 1}$ denote the uplink pilot of UE k , with $\|\mathbf{p}_k^{\text{UL-1}}\|^2 = \tau^{\text{UL-1}}$, $\forall k \in \mathcal{K}$. Each UE k synchronously transmits its pilot $\mathbf{p}_k^{\text{UL-1}}$ using

its scaled combiner \mathbf{v}_k as precoder, i.e.,

$$\mathbf{X}_k^{\text{UL-1}} \triangleq \sqrt{\beta^{\text{UL-1}}} \mathbf{v}_k (\mathbf{p}_k^{\text{UL-1}})^{\text{H}} \in \mathbb{C}^{N \times \tau^{\text{UL-1}}}, \quad (7)$$

where the power scaling factor $\beta^{\text{UL-1}}$ (equal for all the UEs) ensures that $\mathbf{X}_k^{\text{UL-1}}$ complies with the per-UE transmit power constraint. Then, the signal received at BS b is given by

$$\mathbf{Y}_b^{\text{UL-1}} \triangleq \sum_{k \in \mathcal{K}} \mathbf{H}_{b,k} \mathbf{X}_k^{\text{UL-1}} + \mathbf{Z}_b^{\text{UL-1}} = \sqrt{\beta^{\text{UL-1}}} \sum_{k \in \mathcal{K}} \mathbf{h}_{b,k} (\mathbf{p}_k^{\text{UL-1}})^{\text{H}} + \mathbf{Z}_b^{\text{UL-1}} \in \mathbb{C}^{M \times \tau^{\text{UL-1}}}, \quad (8)$$

where $\mathbf{Z}_b^{\text{UL-1}}$ is the AWGN with i.i.d. $\mathcal{CN}(0, \sigma_{\text{BS}}^2)$ elements. Finally, the LS estimate of $\mathbf{h}_{b,k}$ is

$$\hat{\mathbf{h}}_{b,k} \triangleq \frac{1}{\tau^{\text{UL-1}} \sqrt{\beta^{\text{UL-1}}}} \mathbf{Y}_b^{\text{UL-1}} \mathbf{p}_k^{\text{UL-1}} = \mathbf{h}_{b,k} + \frac{1}{\tau^{\text{UL-1}}} \sum_{\bar{k} \neq k} \mathbf{h}_{b,\bar{k}} (\mathbf{p}_{\bar{k}}^{\text{UL-1}})^{\text{H}} \mathbf{p}_k^{\text{UL-1}} + \frac{1}{\tau^{\text{UL-1}} \sqrt{\beta^{\text{UL-1}}}} \mathbf{Z}_b^{\text{UL-1}} \mathbf{p}_k^{\text{UL-1}} \in \mathbb{C}^{M \times 1}. \quad (9)$$

Group-specific effective uplink channel estimation (UL-2). The above antenna-specific and UE-specific channel estimations allow to apply UE-specific weights to the channel estimates at the BSs. To the contrary, in the group-specific channel estimation, the UE-specific weights must be already applied during the pilot transmission. Accordingly, let ω_k be the weight of UE k and let $\mathbf{f}_{b,g} \triangleq \sum_{k \in \mathcal{K}_g} \omega_k \mathbf{H}_{b,k} \mathbf{v}_k \in \mathbb{C}^{M \times 1}$ denote the effective uplink channel between \mathcal{K}_g and BS b . Furthermore, let $\mathbf{p}_g^{\text{UL-2}} \in \mathbb{C}^{\tau^{\text{UL-2}} \times 1}$ be the uplink pilot of group g , with $\|\mathbf{p}_g^{\text{UL-2}}\|^2 = \tau^{\text{UL-2}}$, $\forall g \in \mathcal{G}$. Each UE k synchronously transmits its pilot $\mathbf{p}_{g_k}^{\text{UL-2}}$ using its scaled combiner \mathbf{v}_k as precoder, i.e.,

$$\mathbf{X}_k^{\text{UL-2}} \triangleq \sqrt{\beta^{\text{UL-2}}} \omega_k \mathbf{v}_k (\mathbf{p}_{g_k}^{\text{UL-2}})^{\text{H}} \in \mathbb{C}^{N \times \tau^{\text{UL-2}}}, \quad (10)$$

where the power scaling factor $\beta^{\text{UL-2}}$ (equal for all the UEs) ensures that $\mathbf{X}_k^{\text{UL-2}}$ complies with the per-UE transmit power constraint. Then, the signal received at BS b is given by

$$\mathbf{Y}_b^{\text{UL-2}} \triangleq \sum_{k \in \mathcal{K}} \mathbf{H}_{b,k} \mathbf{X}_k^{\text{UL-2}} + \mathbf{Z}_b^{\text{UL-2}} = \sqrt{\beta^{\text{UL-2}}} \sum_{g \in \mathcal{G}} \mathbf{f}_{b,g} (\mathbf{p}_g^{\text{UL-2}})^{\text{H}} + \mathbf{Z}_b^{\text{UL-2}} \in \mathbb{C}^{M \times \tau^{\text{UL-2}}}, \quad (11)$$

where $\mathbf{Z}_b^{\text{UL-2}}$ is the AWGN with i.i.d. $\mathcal{CN}(0, \sigma_{\text{BS}}^2)$ elements. Finally, the LS estimate of $\mathbf{f}_{b,g}$ is

$$\hat{\mathbf{f}}_{b,g} \triangleq \frac{1}{\tau^{\text{UL-2}} \sqrt{\beta^{\text{UL-2}}}} \mathbf{Y}_b^{\text{UL-2}} \mathbf{p}_g^{\text{UL-2}} = \mathbf{f}_{b,g} + \frac{1}{\tau^{\text{UL-2}}} \sum_{\bar{g} \neq g} \mathbf{f}_{b,\bar{g}} (\mathbf{p}_{\bar{g}}^{\text{UL-2}})^{\text{H}} \mathbf{p}_g^{\text{UL-2}} + \frac{1}{\tau^{\text{UL-2}} \sqrt{\beta^{\text{UL-2}}}} \mathbf{Z}_b^{\text{UL-2}} \mathbf{p}_g^{\text{UL-2}} \in \mathbb{C}^{M \times 1}. \quad (12)$$

Effective downlink channel estimation (DL). Let $\mathbf{g}_k \triangleq \sum_{b \in \mathcal{B}} \mathbf{H}_{b,k}^{\text{H}} \mathbf{w}_{b,g} \in \mathbb{C}^{N \times 1}$ be the effective downlink channel between all the BSs and UE k . Moreover, let $\mathbf{p}_g^{\text{DL}} \in \mathbb{C}^{\tau^{\text{DL}} \times 1}$ denote the downlink pilot of group g , with $\|\mathbf{p}_g^{\text{DL}}\|^2 = \tau^{\text{DL}}$, $\forall g \in \mathcal{G}$. Each BS b synchronously transmits a superposition of the pilots $\{\mathbf{p}_g^{\text{DL}}\}_{g \in \mathcal{G}}$ after precoding them with the corresponding precoders $\{\mathbf{w}_{b,g}\}_{g \in \mathcal{G}}$, i.e.,

$$\mathbf{X}_b^{\text{DL}} \triangleq \sum_{g \in \mathcal{G}} \mathbf{w}_{b,g} (\mathbf{p}_g^{\text{DL}})^{\text{H}} \in \mathbb{C}^{M \times \tau^{\text{DL}}}. \quad (13)$$

Then, the signal received at UE k is given by

$$\mathbf{Y}_k^{\text{DL}} \triangleq \sum_{b \in \mathcal{B}} \mathbf{H}_{b,k}^H \mathbf{X}_b^{\text{DL}} + \mathbf{Z}_k^{\text{DL}} = \sum_{b \in \mathcal{B}} \sum_{g \in \mathcal{G}} \mathbf{H}_{b,k}^H \mathbf{w}_{b,g} (\mathbf{p}_g^{\text{DL}})^H + \mathbf{Z}_k^{\text{DL}} \in \mathbb{C}^{N \times \tau^{\text{DL}}}, \quad (14)$$

where \mathbf{Z}_k^{DL} is the AWGN with i.i.d. $\mathcal{CN}(0, \sigma_{\text{UE}}^2)$ elements. Finally, the LS estimate of \mathbf{g}_k is

$$\hat{\mathbf{g}}_k \triangleq \frac{1}{\tau^{\text{DL}}} \mathbf{Y}_k^{\text{DL}} \mathbf{P}_{g_k}^{\text{DL}} = \mathbf{g}_k + \frac{1}{\tau^{\text{DL}}} \sum_{b \in \mathcal{B}} \sum_{\bar{g} \neq g_k} \mathbf{H}_{b,k}^H \mathbf{w}_{b,\bar{g}} (\mathbf{p}_{\bar{g}}^{\text{DL}})^H \mathbf{P}_{g_k}^{\text{DL}} + \frac{1}{\tau^{\text{DL}}} \mathbf{Z}_k^{\text{DL}} \mathbf{P}_{g_k}^{\text{DL}} \in \mathbb{C}^{N \times 1}. \quad (15)$$

III. PROBLEM FORMULATION

The goal of this paper is to propose fully distributed multi-group multicast precoding designs for cell-free massive MIMO systems based on the MMSE criterion. In this section, we establish the basis for the distributed precoding design by considering the centralized implementation with perfect CSI. First, in Section III-A, we focus on the sum-group MSE minimization and identify several practical challenges with its distributed implementation. Then, in Section III-B, we approximate the sum-group MSE minimization with a weighted sum MSE minimization, based on which we develop the proposed distributed precoding designs presented in Sections IV and V with perfect and imperfect CSI, respectively.

A. Sum-Group MSE Minimization

The sum-group MSE minimization achieves absolute MSE fairness within each multicast group through the min-max MSE criterion subject to the per-BS transmit power constraints. Accordingly, the precoders and combiners are optimized by solving

$$\begin{aligned} & \underset{\{\mathbf{w}_g, \mathbf{v}_k\}}{\text{minimize}} && \sum_{g \in \mathcal{G}} \max_{k \in \mathcal{K}_g} \text{MSE}_k \\ & \text{s.t.} && \sum_{g \in \mathcal{G}} \|\mathbf{E}_b \mathbf{w}_g\|^2 \leq \rho_{\text{BS}}, \quad \forall b \in \mathcal{B}, \end{aligned} \quad (16)$$

where MSE_k is the MSE of UE k defined as

$$\text{MSE}_k \triangleq \mathbb{E} [|\mathbf{v}_k^H \mathbf{y}_k - d_{g_k}|^2] = \sum_{g \in \mathcal{G}} |\mathbf{v}_k^H \mathbf{H}_k^H \mathbf{w}_g|^2 - 2\text{Re}[\mathbf{v}_k^H \mathbf{H}_k^H \mathbf{w}_{g_k}] + \sigma_{\text{UE}}^2 \|\mathbf{v}_k\|^2 + 1, \quad (17)$$

and $\mathbf{E}_b \in \mathbb{R}^{M \times BM}$ is a selection matrix such that $\mathbf{E}_b \mathbf{w}_g = \mathbf{w}_{b,g}$. The problem in (16) is convex with respect to either the precoders or the combiners but not jointly convex with respect to both. Hence, we use *alternating optimization*, whereby the precoders are optimized for fixed combiners and vice versa in an iterative best-response fashion. Before describing each step of the alternating

optimization, let us define $t_g \triangleq \max_{k \in \mathcal{K}_g} \text{MSE}_k$ and rewrite (16) in epigraph form as

$$\begin{aligned} & \underset{\{\mathbf{w}_g, \mathbf{v}_k, t_g\}}{\text{minimize}} && \sum_{g \in \mathcal{G}} t_g \\ & \text{s.t.} && \mu_k : \text{MSE}_k \leq t_g, \quad \forall k \in \mathcal{K}_g, \quad \forall g \in \mathcal{G} \\ & && \lambda_b : \sum_{g \in \mathcal{G}} \|\mathbf{E}_b \mathbf{w}_g\|^2 \leq \rho_{\text{BS}}, \quad \forall b \in \mathcal{B}. \end{aligned} \quad (18)$$

Optimization of the combiners. For a fixed set of precoders $\{\mathbf{w}_g\}_{g \in \mathcal{G}}$, the combiners $\{\mathbf{v}_k\}_{k \in \mathcal{K}}$ are optimized by solving the following convex problem:

$$\begin{aligned} & \underset{\{\mathbf{v}_k, t_g\}}{\text{minimize}} && \sum_{g \in \mathcal{G}} t_g \\ & \text{s.t.} && \text{MSE}_k \leq t_g, \quad \forall k \in \mathcal{K}_g, \quad \forall g \in \mathcal{G}. \end{aligned} \quad (19)$$

The Lagrangian of (19) can be written as

$$\mathcal{L}_{(19)}(\{\mathbf{v}_k, t_g, \mu_k\}) \triangleq \sum_{g \in \mathcal{G}} t_g + \sum_{k \in \mathcal{K}} \mu_k (\text{MSE}_k - t_{g_k}), \quad (20)$$

where μ_k is the dual variable corresponding to each per-UE MSE constraint in (18). Then, the optimal \mathbf{v}_k is obtained by setting $\nabla_{\mathbf{v}_k} \mathcal{L}_{(19)}(\{\mathbf{v}_k, t_g, \mu_k\}) = \mathbf{0}$, which yields

$$\mathbf{v}_k = \left(\sum_{g \in \mathcal{G}} \mathbf{H}_k^H \mathbf{w}_g \mathbf{w}_g^H \mathbf{H}_k + \sigma_{\text{UE}}^2 \mathbf{I}_N \right)^{-1} \mathbf{H}_k^H \mathbf{w}_{g_k}. \quad (21)$$

Optimization of the precoders. For a fixed set of combiners $\{\mathbf{v}_k\}_{k \in \mathcal{K}}$, the precoders $\{\mathbf{w}_g\}_{g \in \mathcal{G}}$ are optimized by solving the following convex problem:

$$\begin{aligned} & \underset{\{\mathbf{w}_g, t_g\}}{\text{minimize}} && \sum_{g \in \mathcal{G}} t_g \\ & \text{s.t.} && \text{MSE}_k \leq t_g, \quad \forall k \in \mathcal{K}_g, \quad \forall g \in \mathcal{G} \\ & && \sum_{g \in \mathcal{G}} \|\mathbf{E}_b \mathbf{w}_g\|^2 \leq \rho_{\text{BS}}, \quad \forall b \in \mathcal{B}, \end{aligned} \quad (22)$$

which can be solved, e.g. via CVX [28]. Alternatively, one can resort to the Karush–Kuhn–Tucker (KKT) conditions, which also conveniently reveal the optimal multi-group multicast precoding structure. In this regard, the Lagrangian of (22) can be written as

$$\mathcal{L}_{(22)}(\{\mathbf{w}_g, t_g, \mu_k, \lambda_b\}) \triangleq \sum_{g \in \mathcal{G}} t_g + \sum_{k \in \mathcal{K}} \mu_k (\text{MSE}_k - t_{g_k}) + \sum_{b \in \mathcal{B}} \lambda_b \left(\sum_{g \in \mathcal{G}} \|\mathbf{E}_b \mathbf{w}_g\|^2 - \rho_{\text{BS}} \right), \quad (23)$$

where λ_b is the dual variable corresponding to each per-BS transmit power constraint in (18).

Then, the optimal \mathbf{w}_g is obtained by setting $\nabla_{\mathbf{w}_g} \mathcal{L}_{(22)}(\{\mathbf{w}_g, t_g, \mu_k, \lambda_b\}) = \mathbf{0}$, which yields

$$\mathbf{w}_g = \left(\sum_{k \in \mathcal{K}} \mu_k \mathbf{H}_k \mathbf{v}_k \mathbf{v}_k^H \mathbf{H}_k^H + \sum_{b \in \mathcal{B}} \lambda_b \mathbf{E}_b^H \mathbf{E}_b \right)^{-1} \sum_{k \in \mathcal{K}_g} \mu_k \mathbf{H}_k \mathbf{v}_k. \quad (24)$$

The above expression of \mathbf{w}_g depends on the dual variables $\{\mu_k\}_{k \in \mathcal{K}}$ and $\{\lambda_b\}_{b \in \mathcal{B}}$. Such dual

variables can be updated iteratively using the sub-gradient method as detailed in Appendix I [6], [29], and their values after convergence are finally used in (24).

From the expression of the aggregated precoder \mathbf{w}_g in (24), it is evident that the BS-specific precoders $\{\mathbf{w}_{b,g}\}_{b \in \mathcal{B}}$ also rely on the dual variables $\{\mu_k\}_{k \in \mathcal{K}}$. To compute each $\mathbf{w}_{b,g}$ locally at BS b , extensive backhaul signaling is required to iteratively update the dual variables $\{\mu_k\}_{k \in \mathcal{K}}$ either at the CPU or at each BS in parallel. To simplify the distributed precoding design, we propose to relax the absolute MSE fairness requirement within each multicast group, which leads to a weighted sum MSE minimization. In the following section, we describe the reformulated problem and the corresponding centralized precoding design with perfect CSI.

B. Weighted Sum MSE Minimization

To circumvent the shortcomings of the original problem formulation described in Section III-A, we approximate the sum-group MSE objective in (16) with a weighted sum MSE objective. Accordingly, the precoders and combiners are optimized by solving

$$\begin{aligned} & \underset{\{\mathbf{w}_g, \mathbf{v}_k\}}{\text{minimize}} && \sum_{k \in \mathcal{K}} \omega_k \text{MSE}_k \\ & \text{s.t.} && \lambda_b : \sum_{g \in \mathcal{G}} \|\mathbf{E}_b \mathbf{w}_g\|^2 \leq \rho_{\text{BS}}, \quad \forall b \in \mathcal{B}, \end{aligned} \quad (25)$$

where we recall that ω_k is the weight of UE k . This choice stems from the fact that the weighted sum MSE metric provides a degree of in-built MSE fairness among all the UEs. Since the problem in (25) is convex with respect to either the precoders or the combiners but not jointly convex with respect to both, we use alternating optimization as in the previous section. For a fixed set of combiners $\{\mathbf{v}_k\}_{k \in \mathcal{K}}$, the precoders $\{\mathbf{w}_g\}_{g \in \mathcal{G}}$ can be optimized, e.g, via CVX [28] or by resorting to the KKT conditions. In this regard, the Lagrangian of (25) can be written as

$$\mathcal{L}_{(25)}(\{\mathbf{w}_g, \lambda_b\}) \triangleq \sum_{k \in \mathcal{K}} \omega_k \text{MSE}_k + \sum_{b \in \mathcal{B}} \lambda_b \left(\sum_{g \in \mathcal{G}} \|\mathbf{E}_b \mathbf{w}_g\|^2 - \rho_{\text{BS}} \right). \quad (26)$$

Then, the optimal \mathbf{w}_g is obtained by setting $\nabla_{\mathbf{w}_g} \mathcal{L}_{(25)}(\{\mathbf{w}_g, \lambda_b\}) = \mathbf{0}$, which yields

$$\mathbf{w}_g = \left(\sum_{k \in \mathcal{K}} \omega_k \mathbf{H}_k \mathbf{v}_k \mathbf{v}_k^H \mathbf{H}_k^H + \sum_{b \in \mathcal{B}} \lambda_b \mathbf{E}_b^H \mathbf{E}_b \right)^{-1} \sum_{k \in \mathcal{K}_g} \omega_k \mathbf{H}_k \mathbf{v}_k. \quad (27)$$

If the optimal dual variables $\{\mu_k\}_{k \in \mathcal{K}}$ of the sum-group MSE minimization were known in advance, one could replace the weights $\{\omega_k\}_{k \in \mathcal{K}}$ in (27) with $\{\mu_k\}_{k \in \mathcal{K}}$ at each alternating optimization iteration, which would lead to the same solution of (24). However, the values of $\{\mu_k\}_{k \in \mathcal{K}}$ cannot be known in advance. Moreover, tuning the weights to match the dual variables at each alternating optimization iteration would produce the same complexity and backhaul signaling overhead of

the original sum-group MSE minimization.¹ To simplify the distributed precoding design, we fix the weights to predetermined values and, specifically, we assume $\omega_k = 1, \forall k \in \mathcal{K}$. Hence, in the following, we refer to (25) simply as sum MSE minimization. Though slightly suboptimal, as demonstrated later, this approach leads to much simpler computation and signaling, and is characterized by faster convergence. Note that, especially at high SNR, the UE-specific rates derived from the sum MSE minimization are close to those obtained with the sum-group MSE minimization. This is formalized in Proposition 1. Furthermore, for a fixed set of precoders $\{\mathbf{w}_g\}_{g \in \mathcal{G}}$, the optimal combiners $\{\mathbf{v}_k\}_{k \in \mathcal{K}}$ for (25) are again obtained as in (21) based on the effective downlink channel estimation described in Section II-A.

Proposition 1. *As $\rho_{\text{BS}} \rightarrow \infty$, i.e., at high SNR, the UE-specific rates obtained with the sum MSE minimization in (25) asymptotically approximate the ones resulting from the sum-group MSE minimization in (16).*

Proof: Without loss of generality, let us consider a single BS and let us define $c_{k\bar{k}} \triangleq \frac{\mathbf{v}_k^H \mathbf{H}_k^H \mathbf{w}_{g_{\bar{k}}}}{\|\mathbf{v}_k\| \|\mathbf{w}_{g_{\bar{k}}}\|}$. Assuming that UE k adopts the MMSE combiner in (21), its MSE can be expressed as $\text{MSE}_k = \frac{1}{1+\gamma_k}$ (cf. (17)). As $\rho_{\text{BS}} \rightarrow \infty$, the precoder in (27) approaches a ZF-like solution, i.e., \mathbf{w}_g is projected onto the nullspace of the effective uplink channels of the UEs $k \notin \mathcal{K}_g$ and matched towards the superposition of the effective uplink channels of the UEs $k \in \mathcal{K}_g$. Thus, considering UE $\bar{k} \notin \mathcal{K}_{g_k}$, the inner product between $\mathbf{w}_{g_{\bar{k}}}$ and the effective uplink channel of UE k tends to zero, which leads to $c_{k\bar{k}} \rightarrow 0, \forall \bar{k} \notin \mathcal{K}_{g_k}$. In this context, all the UEs experience high SINR, and the SINR of UE k can be approximated as (cf. (2))

$$\gamma_k \approx \frac{p_{g_k} c_{kk}^2}{\sigma_{\text{UE}}^2}, \quad (28)$$

where p_g is the transmit power allocated to group g . Finally, when $\omega_k = 1, \forall k \in \mathcal{K}$, the sum MSE minimization in (25) reduces to the following power allocation problem:

$$\begin{aligned} & \underset{\{p_g\}}{\text{minimize}} && \sum_{k \in \mathcal{K}} \frac{\sigma_{\text{UE}}^2}{p_{g_k} c_{kk}^2} \\ & \text{s.t.} && \sum_{g \in \mathcal{G}} p_g \leq \rho_{\text{BS}}. \end{aligned} \quad (29)$$

From the KKT conditions detailed in Appendix II, we obtain the optimal p_g as

$$p_g = \rho_{\text{BS}} \frac{u_g}{\sum_{\bar{g} \in \mathcal{G}} u_{\bar{g}}}, \quad (30)$$

¹To reduce the complexity and backhaul signaling overhead, the values of $\{\omega_k\}_{k \in \mathcal{K}}$ may be updated less frequently, e.g., based on SINR reporting from the UEs.

with $u_g \triangleq \sqrt{\sum_{k \in \mathcal{K}_g} \frac{\sigma_{\text{UE}}^2}{c_{kk}^2}}$. Consequently, the rate difference between UE k and UE \bar{k} at high SNR can be written as

$$\left| \log_2(\gamma_k) - \log_2(\gamma_{\bar{k}}) \right| = \left| \log_2 \left(\frac{u_{gk} c_{kk}^2}{u_{g\bar{k}} c_{\bar{k}\bar{k}}^2} \right) \right|, \quad (31)$$

which is independent of ρ_{BS} . This suggests that all the UE-specific rates increase uniformly with the transmit power. Considering the MSE fairness requirement of (18), it follows that the rate of UE $k \in \mathcal{K}_g$ obtained with the sum-group MSE minimization lies within the minimum and the maximum rates among all the UEs $\bar{k} \in \mathcal{K}_g$ obtained with the sum MSE minimization, i.e.,

$$\min_{\bar{k} \in \mathcal{K}_g} R_{\bar{k}}^{\text{S-MSE}} \leq R_k^{\text{SG-MSE}} \leq \max_{\bar{k} \in \mathcal{K}_g} R_{\bar{k}}^{\text{S-MSE}}, \quad \forall k \in \mathcal{K}_g, \quad (32)$$

where $R_k^{\text{S-MSE}}$ and $R_k^{\text{SG-MSE}}$ indicate the rates of UE k obtained with the sum MSE minimization and with the sum-group MSE minimization, respectively. The asymptotic approximation of the normalized difference between $R_k^{\text{S-MSE}}$ and $R_k^{\text{SG-MSE}}$ is given by

$$\begin{aligned} \lim_{\rho_{\text{BS}} \rightarrow \infty} \frac{|R_k^{\text{S-MSE}} - R_k^{\text{SG-MSE}}|}{R_k^{\text{S-MSE}}} &\leq \lim_{\rho_{\text{BS}} \rightarrow \infty} \frac{|\min_{\bar{k} \in \mathcal{K}_g} R_{\bar{k}}^{\text{S-MSE}} - \max_{\bar{k} \in \mathcal{K}_g} R_{\bar{k}}^{\text{S-MSE}}|}{R_k^{\text{S-MSE}}} \\ &\simeq \lim_{\rho_{\text{BS}} \rightarrow \infty} \frac{|\log_2(\min_{\bar{k} \in \mathcal{K}_g} u_{g\bar{k}} c_{\bar{k}\bar{k}}^2) - \log_2(\max_{\bar{k} \in \mathcal{K}_g} u_{g\bar{k}} c_{\bar{k}\bar{k}}^2)|}{\log_2(\rho_{\text{BS}} u_{gk} c_{kk}^2) - \log_2(\sigma_{\text{UE}}^2 \sum_{\bar{g} \in \mathcal{G}} u_{\bar{g}})} \rightarrow 0, \quad \forall k \in \mathcal{K}_g. \end{aligned} \quad (34)$$

Hence, at high SNR, the UE-specific rates obtained with the sum MSE minimization asymptotically approximate the ones resulting from the sum-group MSE minimization. ■

In the rest of the paper, we focus on the sum MSE minimization in (25) to design the multi-group multicast precoders. Before presenting the proposed distributed precoding designs in Sections IV and V with perfect and imperfect CSI, respectively, we briefly illustrate the reference precoding schemes in the following section.

C. Reference Precoding Schemes

The proposed distributed precoding designs are compared with different reference schemes, namely: *i*) the centralized precoding design, which is referred to in the following as the *Centralized*; and *ii*) the local precoding designs based on MMSE and MF, which are referred to in the following as the *Local MMSE* and *Local MF*, respectively [30].

Centralized precoding design. The practical implementation of the *Centralized* requires the antenna-specific uplink channel estimation (see Section II-A) to enable the computation of the precoders in (27) and the combiners in (21) at the CPU. First, each BS b obtains $\{\hat{\mathbf{H}}_{b,k}\}_{k \in \mathcal{K}}$ and forwards them to the CPU via backhaul signaling. Then, the CPU computes the aggregated

precoders $\{\mathbf{w}_g\}_{g \in \mathcal{G}}$ and the combiners $\{\mathbf{v}_k\}_{k \in \mathcal{K}}$ via alternating optimization by replacing \mathbf{H}_k with $\hat{\mathbf{H}}_k \triangleq [\hat{\mathbf{H}}_{1,k}^T, \dots, \hat{\mathbf{H}}_{B,k}^T]^T \in \mathbb{C}^{BM \times N}$ in (27) and (21), respectively. After convergence, the resulting BS-specific precoders are fed back to the corresponding BSs via backhaul signaling. Finally, the effective downlink channel estimation (see Section II-A) is carried out to allow each UE k to compute its (final) combiner as

$$\mathbf{v}_k = (\mathbf{Y}_k^{\text{DL}} (\mathbf{Y}_k^{\text{DL}})^{\text{H}})^{-1} \mathbf{Y}_k^{\text{DL}} \mathbf{P}_{g_k}^{\text{DL}}. \quad (35)$$

Note that (35) coincides with (21) for perfect CSI, i.e., when $\tau^{\text{DL}} \rightarrow \infty$. The implementation of the *Centralized* is summarized in Algorithm 1 on page 21.

Local precoding designs. To avoid the prohibitive complexity and backhaul signaling of large-scale centralized precoding designs, most works on cell-free massive MIMO assume simple local precoding strategies exploiting the large-antenna regime across the BSs [30]. In this setting, the BS-specific precoders are designed based solely on local CSI, ignoring the contribution from the other BSs. Nevertheless, iterative bi-directional training is required to update the precoders at the BSs based on the combiners at the UEs and vice versa. With perfect CSI, at each bi-directional training iteration, the *Local MMSE* precoder at each BS b is computed as

$$\mathbf{w}_{b,g} = \left(\sum_{k \in \mathcal{K}} \omega_k \mathbf{H}_{b,k} \mathbf{v}_k \mathbf{v}_k^{\text{H}} \mathbf{H}_{b,k}^{\text{H}} + \lambda_b \mathbf{I}_M \right)^{-1} \sum_{k \in \mathcal{K}_g} \omega_k \mathbf{H}_{b,k} \mathbf{v}_k, \quad (36)$$

whereas the corresponding *Local MF* precoder is computed as

$$\mathbf{w}_{b,g} = \frac{1}{\lambda_b} \sum_{k \in \mathcal{K}_g} \omega_k \mathbf{H}_{b,k} \mathbf{v}_k. \quad (37)$$

Note that the dual variable λ_b in (36) and (37) can be easily obtained via bisection. In both cases, each UE k computes its combiner as in (21). The local precoding designs may not converge to a solution of the sum MSE minimization in (25). However, the resulting UE-specific rates improve over the iterations since the combiners are better focused towards the intended signals and increase the accuracy of the effective channel estimation. The practical implementation of the *Local MMSE* and *Local MF* requires, at each bi-directional training iteration, the UE-specific and group-specific effective uplink channel estimations, respectively, as well as the effective downlink channel estimation (see Section II-A). Accordingly, the *Local MMSE* precoder at each BS b is computed as

$$\mathbf{w}_{b,g} = \sqrt{\beta^{\text{UL-1}}} (\mathbf{Y}_b^{\text{UL-1}} \mathbf{\Omega} (\mathbf{Y}_b^{\text{UL-1}})^{\text{H}} + \tau^{\text{UL-1}} (\beta^{\text{UL-1}} \lambda_b - \sigma_{\text{BS}}^2) \mathbf{I}_M)^{-1} \sum_{k \in \mathcal{K}_g} \omega_k \mathbf{Y}_b^{\text{UL-1}} \mathbf{p}_k^{\text{UL-1}}, \quad (38)$$

with $\mathbf{\Omega} \triangleq \text{Diag}(\omega_1, \dots, \omega_K) \in \mathbb{R}^{K \times K}$, whereas the corresponding *Local MF* precoder is computed

as

$$\mathbf{w}_{b,g} = \frac{1}{\lambda_b \tau^{\text{UL-2}} \sqrt{\beta^{\text{UL-2}}}} \mathbf{Y}_b^{\text{UL-2}} \mathbf{P}_g^{\text{UL-2}}. \quad (39)$$

In both cases, each UE k computes its combiner as in (35). In each uplink training instance, the *Local MMSE* requires a minimum of $K \geq G$ orthogonal pilots to obtain $\mathbf{Y}_b^{\text{UL-1}}$ in (8), whereas the *Local MF* requires a minimum of G orthogonal pilots to obtain $\mathbf{Y}_b^{\text{UL-2}}$ in (11). For a fixed number of bi-directional iterations, the *Local MMSE* outperforms the *Local MF* by exploiting the local interference covariance matrix, although it has a higher training overhead.

IV. DISTRIBUTED PRECODING DESIGN WITH PERFECT CSI

In this section, we describe the proposed distributed multi-group multicast precoding designs with perfect CSI and backhaul signaling for the CSI exchange. Their practical implementation with imperfect CSI and without any backhaul signaling for the CSI exchange is presented in Section V. The precoders are optimized locally at each BS by means of either best-response or gradient-based updates, as discussed in the following sections.

A. Best-Response Distributed Precoding Design

In the best-response distributed precoding design, which is referred to in the following as *Distributed BR*, the optimal $\mathbf{w}_{b,g}$ is obtained by setting $\nabla_{\mathbf{w}_{b,g}} \mathcal{L}_{(25)}(\{\mathbf{w}_g, \lambda_b\}) = \mathbf{0}$, which yields

$$\mathbf{w}_{b,g} = \left(\sum_{k \in \mathcal{K}} \omega_k \mathbf{H}_{b,k} \mathbf{v}_k \mathbf{v}_k^H \mathbf{H}_{b,k}^H + \lambda_b \mathbf{I}_M \right)^{-1} \left(\sum_{k \in \mathcal{K}_g} \omega_k \mathbf{H}_{b,k} \mathbf{v}_k - \underbrace{\sum_{\bar{b} \neq b} \sum_{k \in \mathcal{K}} \omega_k \mathbf{H}_{b,k} \mathbf{v}_k \mathbf{v}_k^H \mathbf{H}_{\bar{b},k}^H \mathbf{w}_{\bar{b},g}}_{\triangleq \boldsymbol{\xi}_{b,g} \text{ (cross terms)}} \right). \quad (40)$$

The above precoder can be computed locally at BS b provided that $\boldsymbol{\xi}_{b,g}$, which comprises group-specific cross terms from the other BSs, is known. To reconstruct $\boldsymbol{\xi}_{b,g}$, BS b needs to obtain $\{\mathbf{v}_k^H \mathbf{H}_{\bar{b},k}^H \mathbf{w}_{\bar{b},g}\}_{k \in \mathcal{K}}$ from each BS $\bar{b} \neq b$ via backhaul signaling as in [19]. In practice, each BS is required to share GK complex scalars with the other BSs. In addition, the backhaul signaling introduces a delay that causes each BS to reconstruct the cross terms based on outdated CSI from the other BSs. As done in [20], we assume that such a delay consists of a single bi-directional training iteration. Hence, the cross terms $\boldsymbol{\xi}_{b,g}$ at iteration i are given by $\boldsymbol{\xi}_{b,g}^{(i)} \triangleq \sum_{\bar{b} \neq b} \sum_{k \in \mathcal{K}} \omega_k \mathbf{H}_{b,k} \mathbf{v}_k \mathbf{v}_k^H \mathbf{H}_{\bar{b},k}^H \mathbf{w}_{\bar{b},g}^{(i-1)}$. With this information, all the BSs can compute their precoders simultaneously building on the parallel optimization framework [31], which uses best-response updates to ensure the convergence to a solution of the sum MSE minimization in

(25). Finally, the BS-specific precoder at iteration i is computed as

$$\mathbf{w}_{b,g}^{(i)} = (1 - \alpha_{\text{BR}})\mathbf{w}_{b,g}^{(i-1)} + \alpha_{\text{BR}}\mathbf{w}_{b,g} = \mathbf{w}_{b,g}^{(i-1)} - \underbrace{\alpha_{\text{BR}}(\mathbf{w}_{b,g}^{(i-1)} - \mathbf{w}_{b,g})}_{\triangleq \Delta\mathbf{w}_{b,g}^*}, \quad (41)$$

where the step size $\alpha_{\text{BR}} \in (0, 1]$ strikes a balance between convergence speed and accuracy of the solution [31], and $\Delta\mathbf{w}_{b,g}^*$ is obtained by replacing $\boldsymbol{\xi}_{b,g}$ with $\boldsymbol{\xi}_{b,g}^{(i)}$ in (40), i.e.,

$$\begin{aligned} \Delta\mathbf{w}_{b,g}^* = & - \left(\sum_{k \in \mathcal{K}} \omega_k \mathbf{H}_{b,k} \mathbf{v}_k \mathbf{v}_k^H \mathbf{H}_{b,k}^H + \lambda_b \mathbf{I}_M \right)^{-1} \left(\sum_{k \in \mathcal{K}_g} \omega_k \mathbf{H}_{b,k} \mathbf{v}_k \right. \\ & \left. - \sum_{\bar{b} \in \mathcal{B}} \sum_{k \in \mathcal{K}} \omega_k \mathbf{H}_{b,k} \mathbf{v}_k \mathbf{v}_k^H \mathbf{H}_{\bar{b},k}^H \mathbf{w}_{\bar{b},g}^{(i-1)} - \lambda_b \mathbf{w}_{b,g}^{(i-1)} \right) \in \mathbb{C}^{M \times 1}. \end{aligned} \quad (42)$$

Theorem 1. $\Delta\mathbf{w}_{b,g}^*$ in (42) is a steepest descent direction for the sum MSE minimization in (25).

Proof: Let us write the gradient of (26) with respect to $\mathbf{w}_{b,g}$ as

$$\nabla_{\mathbf{w}_{b,g}} \mathcal{L}_{(25)}(\{\mathbf{w}_g, \lambda_b\}) = -2 \left(\sum_{k \in \mathcal{K}_g} \omega_k \mathbf{H}_{b,k} \mathbf{v}_k - \sum_{\bar{b} \in \mathcal{B}} \sum_{k \in \mathcal{K}} \omega_k \mathbf{H}_{b,k} \mathbf{v}_k \mathbf{v}_k^H \mathbf{H}_{\bar{b},k}^H \mathbf{w}_{\bar{b},g} - \lambda_b \mathbf{w}_{b,g} \right). \quad (43)$$

Furthermore, let us define $\mathbf{C}_b \triangleq 2 \left(\sum_{k \in \mathcal{K}} \omega_k \mathbf{H}_{b,k} \mathbf{v}_k \mathbf{v}_k^H \mathbf{H}_{b,k}^H + \lambda_b \mathbf{I}_M \right) \in \mathbb{C}^{M \times M}$ and $\mathbf{C} \triangleq \text{blkdiag}(\mathbf{C}_1, \dots, \mathbf{C}_B) \in \mathbb{C}^{BM \times BM}$. Then, we simplify (42) as

$$\Delta\mathbf{w}_{b,g}^* = \mathbf{C}_b^{-1} \nabla_{\mathbf{w}_{b,g}} \mathcal{L}_{(25)}(\{\mathbf{w}_g, \lambda_b\}) \quad (44)$$

and, exploiting the fact that $\mathbf{C}^{-1} = \text{blkdiag}(\mathbf{C}_1^{-1}, \dots, \mathbf{C}_B^{-1})$, we have

$$\Delta\mathbf{w}_g^* \triangleq [(\Delta\mathbf{w}_{1,g}^*)^T, \dots, (\Delta\mathbf{w}_{B,g}^*)^T]^T = \mathbf{C}^{-1} \nabla_{\mathbf{w}_g} \mathcal{L}_{(25)}(\{\mathbf{w}_g, \lambda_b\}) \in \mathbb{C}^{BM \times 1}. \quad (45)$$

Finally, we observe that $\Delta\mathbf{w}_g^*$ in (45) is a steepest descent direction for the quadratic norm $\|\mathbf{x}\|_{\mathbf{C}} \triangleq (\mathbf{x}^H \mathbf{C} \mathbf{x})^{\frac{1}{2}}$ [32]. ■

Remark 1. Theorem 1 states that, for a fixed set of combiners $\{\mathbf{v}_k\}_{k \in \mathcal{K}}$, the *Distributed BR* solves the sum MSE minimization in (25) via a steepest descent method characterized by the quadratic norm $\|\mathbf{x}\|_{\mathbf{C}}$. Since \mathbf{C} is a block-diagonal matrix with blocks $\{\mathbf{C}_b\}_{b \in \mathcal{B}}$, each BS b greedily aims to reduce its individual MSE by following the steepest descent direction for the quadratic norm $\|\mathbf{x}\|_{\mathbf{C}_b}$, whereas the convergence to a solution of the sum MSE minimization is guaranteed by a proper choice of α_{BR} . On the other hand, the centralized precoding design with best-response updates is obtained by replacing \mathbf{C} with the Hessian of (26) in (45), where the latter is a full matrix. Therefore, the *Distributed BR* is not equivalent to its centralized implementation and, as a consequence, may be characterized by slow convergence. This motivates the development of the gradient-based distributed precoding design in Section IV-B. Lastly, we note that the outdated

CSI used to reconstruct the cross terms at each BS further slows down the convergence.

Remark 2. To speed up the convergence of the *Distributed BR*, we impose that, for a fixed set of combiners $\{\mathbf{v}_k\}_{k \in \mathcal{K}}$, the BS-specific precoders $\{\mathbf{w}_{b,g}\}_{g \in \mathcal{G}}$ are updated only once at each BS b . In this respect, a sufficiently small α_{BR} would ensure the monotonic (yet slow) convergence to a solution of the sum MSE minimization in (25) even with a single update of the precoders for a fixed set of combiners [31]. However, considering a practical scenario where only a limited number of bi-directional training iterations is admissible, we disregard the strictly monotonic convergence and choose α_{BR} to promote an aggressive reduction of the sum MSE objective during the first few iterations.

B. Gradient-Based Distributed Precoding Design

The *Distributed BR* presented in Section IV-A is not equivalent to its centralized implementation and may be thus characterized by slow convergence (see Remark 1). Hence, in this section, we propose a gradient-based distributed precoding design, which is referred to in the following as *Distributed GB* and follows directly from its centralized implementation. In this method, the BS-specific precoders are first updated using the gradient of the sum MSE objective and then projected to meet the per-BS transmit power constraints. To this end, we write the gradient of the sum MSE objective (cf. (17)) with respect to $\mathbf{w}_{b,g}$ as

$$\nabla_{\mathbf{w}_{b,g}} \left(\sum_{k \in \mathcal{K}} \omega_k \text{MSE}_k \right) = -2 \left(\sum_{k \in \mathcal{K}_g} \omega_k \mathbf{H}_{b,k} \mathbf{v}_k - \sum_{\bar{b} \in \mathcal{B}} \sum_{k \in \mathcal{K}} \omega_k \mathbf{H}_{b,k} \mathbf{v}_k \mathbf{v}_k^H \mathbf{H}_{\bar{b},k}^H \mathbf{w}_{\bar{b},g} \right). \quad (46)$$

Then, the corresponding gradient-based update can be expressed as

$$\tilde{\mathbf{w}}_{b,g}^{(i)} \triangleq \mathbf{w}_{b,g}^{(i-1)} - \alpha_{\text{GB}} \nabla_{\mathbf{w}_{b,g}} \left(\sum_{k \in \mathcal{K}} \omega_k \text{MSE}_k \right) \quad (47)$$

$$= \mathbf{w}_{b,g}^{(i-1)} + 2\alpha_{\text{GB}} \left(\sum_{k \in \mathcal{K}_g} \omega_k \mathbf{H}_{b,k} \mathbf{v}_k - \boldsymbol{\xi}_{b,g}^{(i)} - \sum_{k \in \mathcal{K}} \omega_k \mathbf{H}_{b,k} \mathbf{v}_k \mathbf{v}_k^H \mathbf{H}_{b,k}^H \mathbf{w}_{b,g}^{(i-1)} \right), \quad (48)$$

where α_{GB} is the step size. The above gradient-based update can be computed locally at BS b upon receiving the CSI from the other BSs (necessary to reconstruct the cross terms) via backhaul signaling. Finally, the BS-specific precoders at iteration i are obtained by projecting $\{\tilde{\mathbf{w}}_{b,g}^{(i)}\}_{g \in \mathcal{G}}$ to meet the per-BS transmit power constraint, i.e.,

$$[\mathbf{w}_{b,1}^{(i)}, \dots, \mathbf{w}_{b,G}^{(i)}] = \underset{\{\mathbf{w}_{b,\bar{g}}\}_{\bar{g} \in \mathcal{G}}: \sum_{\bar{g} \in \mathcal{G}} \|\mathbf{w}_{b,\bar{g}}\|^2 \leq \rho_{\text{BS}}}{\text{argmin}} \sum_{\bar{g} \in \mathcal{G}} \|\mathbf{w}_{b,\bar{g}} - \tilde{\mathbf{w}}_{b,\bar{g}}^{(i)}\|^2 = a_b [\tilde{\mathbf{w}}_{b,1}^{(i)}, \dots, \tilde{\mathbf{w}}_{b,G}^{(i)}], \quad (49)$$

with $a_b = \sqrt{\frac{\rho_{\text{BS}}}{\sum_{\bar{g} \in \mathcal{G}} \|\tilde{\mathbf{w}}_{b,\bar{g}}^{(i)}\|^2}}$ if $\sum_{\bar{g} \in \mathcal{G}} \|\tilde{\mathbf{w}}_{b,\bar{g}}^{(i)}\|^2 \geq \rho_{\text{BS}}$ and $a_b = 1$ otherwise. Note that this approach can be easily extended to a unicasting scenario considering a single UE in each multicast group.

Theorem 2. *The Distributed GB is equivalent to its centralized implementation.*

Proof: Considering the centralized implementation, the gradient of the sum MSE objective (cf. (17)) with respect to \mathbf{w}_g is given by

$$\nabla_{\mathbf{w}_g} \left(\sum_{k \in \mathcal{K}} \omega_k \text{MSE}_k \right) = -2 \left(\sum_{k \in \mathcal{K}_g} \omega_k \mathbf{H}_k \mathbf{v}_k - \sum_{k \in \mathcal{K}} \omega_k \mathbf{H}_k \mathbf{v}_k \mathbf{v}_k^H \mathbf{H}_k^H \mathbf{w}_g \right) \quad (50)$$

$$= \left[\left(\nabla_{\mathbf{w}_{1,g}} \left(\sum_{k \in \mathcal{K}} \omega_k \text{MSE}_k \right) \right)^T, \dots, \left(\nabla_{\mathbf{w}_{B,g}} \left(\sum_{k \in \mathcal{K}} \omega_k \text{MSE}_k \right) \right)^T \right]^T, \quad (51)$$

which corresponds to the concatenation of the gradients with respect to the BS-specific precoders (see (46)). As a consequence, the gradient-based update of \mathbf{w}_g can be expressed as the concatenation of the gradient-based updates of the BS-specific precoders (see (48)) at iteration i . Then, the aggregated precoders at iteration i are obtained by projecting the aforementioned gradient-based updates to meet the per-BS transmit power constraints, i.e.,

$$[\mathbf{w}_1^{(i)}, \dots, \mathbf{w}_G^{(i)}] = \underset{\{\mathbf{w}_{b,\bar{g}}\}_{\bar{g} \in \mathcal{G}: \sum_{\bar{g} \in \mathcal{G}} \|\mathbf{w}_{b,\bar{g}}\|^2 \leq \rho_{\text{BS}}\}_{b \in \mathcal{B}}}}{\text{argmin}} \sum_{b \in \mathcal{B}} \sum_{\bar{g} \in \mathcal{G}} \|\mathbf{w}_{b,\bar{g}} - \tilde{\mathbf{w}}_{b,\bar{g}}^{(i)}\|^2 = \begin{bmatrix} a_1 [\tilde{\mathbf{w}}_{1,1}^{(i)}, \dots, \tilde{\mathbf{w}}_{1,G}^{(i)}] \\ \vdots \\ a_B [\tilde{\mathbf{w}}_{B,1}^{(i)}, \dots, \tilde{\mathbf{w}}_{B,G}^{(i)}] \end{bmatrix}. \quad (52)$$

Finally, we observe that the aggregated precoders in (52) correspond to the concatenation of the BS-specific precoders in (49). ■

Remark 3. Theorem 2 states that, for a fixed set of combiners $\{\mathbf{v}_k\}_{k \in \mathcal{K}}$, the *Distributed GB* (where the BS-specific precoders $\{\mathbf{w}_{b,g}\}_{g \in \mathcal{G}}$ are optimized locally at each BS b) solves the sum MSE minimization problem in (25) in the same way as its centralized implementation (where the aggregated precoders $\{\mathbf{w}_g\}_{g \in \mathcal{G}}$ are optimized at the CPU). Therefore, each BS directly targets to reduce the sum MSE rather than its individual MSE as in the *Distributed BR*. Moreover, the convergence to a solution of the sum MSE minimization is guaranteed by a proper choice of α_{GB} . Lastly, the comments in Remark 2 on how to speed up the convergence of the *Distributed BR* also apply here.

V. DISTRIBUTED PRECODING DESIGN WITH PILOT-AIDED CHANNEL ESTIMATION

In this section, we describe the practical implementation of the proposed distributed multi-group multicast precoding designs with imperfect CSI and without any backhaul signaling for the CSI exchange. The local computation of the precoders at each BS in (40) relies on group-specific cross terms from the other BSs. To avoid the resulting CSI exchange via backhaul signaling, we

adopt an OTA signaling scheme similar to that proposed in our previous works on distributed precoding design for cell-free massive MIMO unicasting [20], [25]. Therein, we introduced a UE-specific OTA uplink training resource to eliminate the need for backhaul signaling to exchange the UE-specific CSI. In this paper, we propose a new group-specific OTA uplink training resource tailored for the multi-group multicasting scenario, which eliminates the need for backhaul signaling to exchange the group-specific CSI.

New Group-specific OTA uplink training resource (UL-3). To reconstruct the cross terms $\xi_{b,g}$ locally at BS b , each UE k transmits \mathbf{Y}_k^{DL} in (14) after precoding it with $\omega_k \mathbf{v}_k \mathbf{v}_k^{\text{H}}$, i.e.,

$$\mathbf{X}_k^{\text{UL-3}} \triangleq \sqrt{\beta^{\text{UL-3}}} \omega_k \mathbf{v}_k \mathbf{v}_k^{\text{H}} \mathbf{Y}_k^{\text{DL}} \in \mathbb{C}^{N \times \tau^{\text{DL}}}, \quad (53)$$

where the power scaling factor $\sqrt{\beta^{\text{UL-3}}}$ (equal for all the UEs) ensures that $\mathbf{X}_k^{\text{UL-3}}$ complies with the per-UE transmit power constraint. We observe that (53) contains the group-specific effective downlink channels between all the BSs and UE k , and we recall that \mathbf{Y}_k^{DL} is obtained by means of group-specific pilots (see Section II-A). Therefore, this new OTA uplink training resource generates the same training overhead as the effective downlink channel estimation, which depends on G rather than K as in the unicasting scenario. Then, the signal received at BS b is given by

$$\mathbf{Y}_b^{\text{UL-3}} \triangleq \sum_{k \in \mathcal{K}} \omega_k \mathbf{H}_{b,k} \mathbf{v}_k \mathbf{v}_k^{\text{H}} \mathbf{Y}_k^{\text{DL}} + \mathbf{Z}_k^{\text{UL-3}} \quad (54)$$

$$= \sqrt{\beta^{\text{UL-3}}} \sum_{k \in \mathcal{K}} \omega_k \mathbf{H}_{b,k} \mathbf{v}_k \mathbf{v}_k^{\text{H}} \left(\sum_{g \in \mathcal{G}} \mathbf{H}_k^{\text{H}} \mathbf{w}_g (\mathbf{p}_g^{\text{DL}})^{\text{H}} + \mathbf{Z}_k^{\text{DL}} \right) + \mathbf{Z}_k^{\text{UL-3}} \in \mathbb{C}^{M \times \tau^{\text{DL}}}, \quad (55)$$

where $\mathbf{Z}_b^{\text{UL-3}} \in \mathbb{C}^{M \times \tau^{\text{DL}}}$ is the AWGN with i.i.d. $\mathcal{CN}(0, \sigma_{\text{BS}}^2)$ elements. Finally, the LS estimate of $\xi_{b,g}$ is

$$\hat{\xi}_{b,g} \triangleq \frac{1}{\tau^{\text{DL}} \sqrt{\beta^{\text{UL-3}}}} \mathbf{Y}_b^{\text{UL-3}} \mathbf{p}_g^{\text{DL}} \quad (56)$$

$$= \xi_{b,g} + \frac{1}{\tau^{\text{DL}}} \left(\sum_{\bar{g} \neq g} \xi_{b,\bar{g}} (\mathbf{p}_{\bar{g}}^{\text{DL}})^{\text{H}} + \sum_{k \in \mathcal{K}} \omega_k \mathbf{H}_{b,k} \mathbf{v}_k \mathbf{v}_k^{\text{H}} \mathbf{Z}_k^{\text{DL}} + \frac{1}{\sqrt{\beta^{\text{UL-3}}}} \mathbf{Z}_k^{\text{UL-3}} \right) \mathbf{p}_g^{\text{DL}} \in \mathbb{C}^{M \times 1}. \quad (57)$$

A. Best-Response Distributed Precoding Design

The practical implementation of the *Distributed BR* requires, at each bi-directional training iteration, the UE-specific effective uplink channel estimation and the effective downlink channel estimation (see Section II-A) together with the new group-specific OTA uplink training resource (see Section V). In this setting, $\mathbf{Y}_b^{\text{UL-1}}$ in (8) and $\mathbf{Y}_b^{\text{UL-3}}$ in (55) are suitably combined to reconstruct

$\Delta \mathbf{w}_{b,g}^*$ in (42) as

$$\begin{aligned} \Delta \mathbf{w}_{b,g}^* \simeq & - \left(\mathbf{Y}_b^{\text{UL-1}} \boldsymbol{\Omega} (\mathbf{Y}_b^{\text{UL-1}})^{\text{H}} + \tau^{\text{UL-1}} (\beta^{\text{UL-1}} \lambda_b - \sigma_{\text{BS}}^2) \mathbf{I}_M \right)^{-1} \left(\sqrt{\beta^{\text{UL-1}}} \sum_{k \in \mathcal{K}_g} \omega_k \mathbf{Y}_b^{\text{UL-1}} \mathbf{p}_k^{\text{UL-1}} \right. \\ & \left. - \frac{\tau^{\text{UL-1}} \beta^{\text{UL-1}}}{\tau^{\text{DL}} \sqrt{\beta^{\text{UL-3}}}} \mathbf{Y}_b^{\text{UL-3}} (\mathbf{p}_g^{\text{DL}})^{\text{H}} - \beta^{\text{UL-1}} \tau^{\text{UL-1}} \lambda_b \mathbf{w}_{b,g}^{(i-1)} \right), \end{aligned} \quad (58)$$

which is used to compute the BS-specific precoder in (41). Note that (58) becomes equal to (42) with perfect CSI, i.e., when $\tau^{\text{UL-1}} \rightarrow \infty$ and $\tau^{\text{DL}} \rightarrow \infty$. In each uplink training instance, the *Distributed BR* requires a minimum of $K + G$ orthogonal pilots, i.e., K orthogonal pilots to obtain $\mathbf{Y}_b^{\text{UL-1}}$ in (8) and G orthogonal pilots to obtain $\mathbf{Y}_b^{\text{UL-3}}$ in (55). The implementation of the *Distributed BR* is summarized in Algorithm 2 on page 21.

B. Best-Response Distributed Precoding Design with Group-Specific Pilots

The practical implementation of the *Distributed BR* described in Section V-A relies on the UE-specific effective uplink channel estimation, which requires a minimum of K orthogonal pilots in each uplink training instance. To reduce the training overhead, we propose a best-response distributed precoding design based solely on group-specific pilots, which is referred to in the following as the *Distributed BR-GS*. This method is obtained by replacing the UE-specific effective uplink channel estimation with its group-specific counterpart (see Section II-A). Consequently, in each uplink training instance, the *Distributed BR-GS* requires a minimum of $2G < K + G$ orthogonal pilots, i.e., G orthogonal pilots to obtain $\mathbf{Y}_b^{\text{UL-2}}$ in (11) and G orthogonal pilots to obtain $\mathbf{Y}_b^{\text{UL-3}}$ in (55). In this setting, assuming $\omega_k = 1$, $\forall k \in \mathcal{K}$, $\mathbf{Y}_b^{\text{UL-2}}$ in (11) and $\mathbf{Y}_b^{\text{UL-3}}$ in (55) are suitably combined to reconstruct $\Delta \mathbf{w}_{b,g}^*$ in (42) as

$$\begin{aligned} \Delta \mathbf{w}_{b,g}^* \simeq & - \left(\mathbf{Y}_b^{\text{UL-2}} (\mathbf{Y}_b^{\text{UL-2}})^{\text{H}} + \tau^{\text{UL-2}} (\beta^{\text{UL-2}} \lambda_b - \sigma_{\text{BS}}^2) \mathbf{I}_M \right)^{-1} \\ & \times \left(\sqrt{\beta^{\text{UL-2}}} \mathbf{Y}_b^{\text{UL-2}} \mathbf{p}_g^{\text{UL-2}} - \frac{\beta^{\text{UL-2}} \tau^{\text{UL-2}}}{\sqrt{\beta^{\text{UL-3}} \tau^{\text{DL}}}} \mathbf{Y}_b^{\text{UL-3}} (\mathbf{p}_g^{\text{DL}})^{\text{H}} - \beta^{\text{UL-2}} \tau^{\text{UL-2}} \lambda_b \mathbf{w}_{b,g}^{(i-1)} \right), \end{aligned} \quad (59)$$

which is used to compute the BS-specific precoder in (41). To understand the convergence behavior of the *Distributed BR-GS*, let us assume for a moment that perfect CSI is available at BS b , i.e., $\tau^{\text{UL-2}} \rightarrow \infty$ and $\tau^{\text{DL}} \rightarrow \infty$. In this case, we have

$$\Delta \mathbf{w}_{b,g}^* \simeq \mathbf{D}_b^{-1} \nabla_{\mathbf{w}_{b,g}} \mathcal{L}_{(25)}(\{\mathbf{w}_g, \lambda_b\}) \quad (60)$$

with $\nabla_{\mathbf{w}_{b,g}} \mathcal{L}_{(25)}(\{\mathbf{w}_g, \lambda_b\})$ given in (43) and

$$\mathbf{D}_b \triangleq 2 \left(\sum_{k \in \mathcal{K}} \mathbf{H}_{b,k} \mathbf{v}_k \mathbf{v}_k^{\text{H}} \mathbf{H}_{b,k}^{\text{H}} + \underbrace{\sum_{\bar{g} \in \mathcal{G}} \left(\sum_{k \in \mathcal{K}_{\bar{g}}} \mathbf{H}_{b,k} \mathbf{v}_k \right) \left(\sum_{\bar{k} \in \mathcal{K}_{\bar{g}} \setminus \{k\}} \mathbf{v}_{\bar{k}}^{\text{H}} \mathbf{H}_{b,\bar{k}}^{\text{H}} \right)}_{\text{extra interference}} + \lambda_b \mathbf{I}_M \right). \quad (61)$$

We observe that (60) includes an extra interference term with respect to (42), which arises from reconstructing the local interference covariance matrix based solely on group-specific CSI (i.e., $\mathbf{Y}_b^{\text{UL-2}}$ in (11)) rather than UE-specific CSI (i.e., $\mathbf{Y}_b^{\text{UL-1}}$ in (8)) as in (58) for the *Distributed BR*. The implementation of the *Distributed BR-GS* is summarized in Algorithm 3 on page 21.

Theorem 3. $\Delta \mathbf{w}_{b,g}^*$ in (60) is a steepest descent direction for the sum MSE minimization in (25).

Proof: The proof follows similar steps to the proof of Theorem 1 and is thus omitted. ■

Remark 4. Following similar arguments to Remark 1, Theorem 3 states that, for a fixed set of combiners $\{\mathbf{v}_k\}_{k \in \mathcal{K}}$, the *Distributed BR-GS* solves the sum MSE minimization in (25) via a steepest descent method characterized by the quadratic norm $\|\mathbf{x}\|_{\mathbf{D}}$, with $\mathbf{D} \triangleq \text{blkdiag}(\mathbf{D}_1, \dots, \mathbf{D}_B) \in \mathbb{C}^{BM \times BM}$. Due to the extra interference term in (60), the *Distributed BR-GS* may be characterized by slower convergence than the *Distributed BR*. Nonetheless, as shown in Section VI, this drawback may be well compensated by the reduced training overhead, especially for short resource blocks. Hence, the *Distributed BR-GS* may outperform the *Distributed BR* in terms of effective sum-group rate. Lastly, the comments in Remark 2 on how to speed up the convergence of the *Distributed BR* also apply here.

C. Gradient-Based Distributed Precoding Design

The practical implementation of the *Distributed GB* requires, at each bi-directional training iteration, the group-specific effective uplink channel estimation and the effective downlink channel estimation (see Section II-A) together with the new group-specific OTA uplink training resource (see Section V). In this setting, $\mathbf{Y}_b^{\text{UL-2}}$ in (11) and $\mathbf{Y}_b^{\text{UL-3}}$ in (55) are suitably combined to reconstruct $\nabla_{\mathbf{w}_{b,g}} \left(\sum_{k \in \mathcal{K}} \omega_k \text{MSE}_k \right)$ in (46) as

$$\nabla_{\mathbf{w}_{b,g}} \left(\sum_{k \in \mathcal{K}} \omega_k \text{MSE}_k \right) \simeq \frac{2}{\tau^{\text{DL}} \sqrt{\beta^{\text{UL-3}}}} \mathbf{Y}_b^{\text{UL-3}} \mathbf{P}_g^{\text{DL}} - \frac{2}{\tau^{\text{UL-2}} \sqrt{\beta^{\text{UL-2}}}} \mathbf{Y}_b^{\text{UL-2}} \mathbf{P}_g^{\text{UL-2}}, \quad (62)$$

which is used to compute the corresponding gradient-based update in (48). Note that (62) becomes equal to (46) with perfect CSI, i.e., when $\tau^{\text{UL-1}} \rightarrow \infty$ and $\tau^{\text{DL}} \rightarrow \infty$. Finally, the BS-specific precoders are obtained by projecting the gradient-based updates to meet the per-BS transmit power constraint as in (49). Remarkably, the *Distributed GB* can be implemented based solely on group-specific pilots. Consequently, in each uplink training instance, the *Distributed GB* requires a minimum of $2G$ orthogonal pilots as the *Distributed BR-GS*. Another significant advantage of the *Distributed GB* is that the computation of the precoders does not involve any matrix inversion,

Algorithm 1 (Centralized)

Data: Pilots $\{\mathbf{P}_k^{\text{UL}}\}_{k \in \mathcal{K}}$ and $\{\mathbf{p}_g^{\text{DL}}\}_{g \in \mathcal{G}}$.

- 1) **UL:** Each UE k transmits \mathbf{X}_k^{UL} in (4); each BS b receives \mathbf{Y}_b^{UL} in (5).
- 2) Each BS b obtains $\{\hat{\mathbf{H}}_{b,k}\}_{k \in \mathcal{K}}$ in (6) and forwards them to the CPU via backhaul signaling.

Initialization: Combiners $\{\mathbf{v}_k\}_{k \in \mathcal{K}}$.

Until a predefined termination criterion is satisfied, **do:**

- 3) The CPU computes the precoders $\{\mathbf{w}_g\}_g$ as in (24) and the combiners $\{\mathbf{v}_k\}_{k \in \mathcal{K}}$ as in (21) by replacing $\{\mathbf{H}_k\}_{k \in \mathcal{K}}$ with $\{\hat{\mathbf{H}}_k\}_{k \in \mathcal{K}}$.

End

- 4) The CPU forwards the resulting BS-specific precoders to the corresponding BSs via backhaul signaling.
 - 5) **DL:** Each BS b transmits \mathbf{X}_b^{DL} in (13); each UE k receives \mathbf{Y}_k^{DL} in (14).
 - 6) Each UE k computes its combiner \mathbf{v}_k as in (35).
-

Algorithm 2 (Distributed BR)

Data: Pilots $\{\mathbf{p}_k^{\text{UL-1}}\}_{k \in \mathcal{K}}$ and $\{\mathbf{p}_g^{\text{DL}}\}_{g \in \mathcal{G}}$.

Initialization: Combiners $\{\mathbf{v}_k\}_{k \in \mathcal{K}}$.

Until a predefined termination criterion is satisfied, **do:**

- 1) **UL-1:** Each UE k transmits $\mathbf{X}_k^{\text{UL-1}}$ in (7); each BS b receives $\mathbf{Y}_b^{\text{UL-1}}$ in (8).
- 2) **UL-3:** Each UE k transmits $\mathbf{X}_k^{\text{UL-3}}$ in (53); each BS b receives $\mathbf{Y}_b^{\text{UL-3}}$ in (55).
- 3) Each BS b reconstructs $\{\Delta \mathbf{w}_{b,g}^*\}_{g \in \mathcal{G}}$ as in (58) and computes the precoders $\{\mathbf{w}_{b,g}\}_{g \in \mathcal{G}}$ as in (41).
- 4) **DL:** Each BS b transmits \mathbf{X}_b^{DL} in (13); each UE k receives \mathbf{Y}_k^{DL} in (14).
- 5) Each UE k computes its combiner \mathbf{v}_k as in (35).

End

Algorithm 3 (Distributed BR-GS)

Data: Pilots $\{\mathbf{p}_g^{\text{UL-2}}\}_{g \in \mathcal{G}}$ and $\{\mathbf{p}_g^{\text{DL}}\}_{g \in \mathcal{G}}$.

Initialization: Combiners $\{\mathbf{v}_k\}_{k \in \mathcal{K}}$.

Until a predefined termination criterion is satisfied, **do:**

- 1) **UL-2:** Each UE k transmits $\mathbf{X}_k^{\text{UL-2}}$ in (10); each BS b receives $\mathbf{Y}_b^{\text{UL-2}}$ as in (11).
- 2) **UL-3:** Each UE k transmits $\mathbf{X}_k^{\text{UL-3}}$ in (53); each BS b receives $\mathbf{Y}_b^{\text{UL-3}}$ as in (55).
- 3) Each BS b reconstructs $\{\Delta \mathbf{w}_{b,g}^*\}_{g \in \mathcal{G}}$ as in (59) and computes the precoders $\{\mathbf{w}_{b,g}\}_{g \in \mathcal{G}}$ as in (41).
- 4) **DL:** Each BS b transmits \mathbf{X}_b^{DL} in (13); each UE k receives \mathbf{Y}_k^{DL} in (14).
- 5) Each UE k computes its combiner \mathbf{v}_k as in (35).

End

Algorithm 4 (Distributed GB)

Data: Pilots $\{\mathbf{p}_g^{\text{UL-2}}\}_{g \in \mathcal{G}}$ and $\{\mathbf{p}_g^{\text{DL}}\}_{g \in \mathcal{G}}$.

Initialization: Combiners $\{\mathbf{v}_k\}_{k \in \mathcal{K}}$.

Until a predefined termination criterion is satisfied, **do:**

- 1) **UL-2:** Each UE k transmits $\mathbf{X}_k^{\text{UL-2}}$ in (10); each BS b receives $\mathbf{Y}_b^{\text{UL-2}}$ as in (11).
- 2) **UL-3:** Each UE k transmits $\mathbf{X}_k^{\text{UL-3}}$ in (53); each BS b receives $\mathbf{Y}_b^{\text{UL-3}}$ as in (55).
- 3) Each BS b reconstructs the gradient of the sum MSE objective with respect to $\{\mathbf{w}_{b,g}\}_{g \in \mathcal{G}}$ as in (62), computes the corresponding gradient-based updates in (48), and projects them as in (49).
- 4) **DL:** Each BS b transmits \mathbf{X}_b^{DL} in (13); each UE k receives \mathbf{Y}_k^{DL} in (14).
- 5) Each UE k computes its combiner \mathbf{v}_k as in (35).

End

which yields a reduced computational complexity with respect to the *Distributed BR* and the *Distributed BR-GS*. The implementation of the *Distributed GB* is summarized in Algorithm 4.

D. Bi-directional Training Implementation Aspects

The practical implementation of the proposed distributed precoding designs requires, at each bi-directional training iteration, the UE-specific or group-specific effective uplink channel estimation and the effective downlink channel estimation (see Section II-A). In addition, they also rely on the new group-specific OTA uplink training resource (see Section V), which eliminates the

Algorithm	UL (τ^{UL})	UL-1 ($\tau^{\text{UL-1}}$)	UL-2 ($\tau^{\text{UL-2}}$)	UL-3 (τ^{DL})	DL (τ^{DL})	Total
<i>Centralized</i> (reference)	KN	–	–	–	G	$KN + G$
<i>Local MMSE</i> (reference)	–	K	–	–	G	$(K + G)I$
<i>Local MF</i> (reference)	–	–	G	–	G	$2GI$
<i>Distributed BR</i> (proposed)	–	K	–	G	G	$(K + 2G)I$
<i>Distributed BR-GS</i> (proposed)	–	–	G	G	G	$3GI$
<i>Distributed GB</i> (proposed)	–	–	G	G	G	$3GI$

Table I: Minimum number of pilot symbols necessary for the iterative bi-directional training in the different algorithms, where I denotes the total number of bi-directional training iterations.

need for backhaul signaling to exchange the group-specific CSI. Consequently, in each uplink training instance, each UE k transmits $\mathbf{X}_k^{\text{UL-1}}$ in (7) or $\mathbf{X}_k^{\text{UL-2}}$ in (10) together with $\mathbf{X}_k^{\text{UL-3}}$ in (53). Similarly, in each downlink training instance, each BS b transmits \mathbf{X}_b^{DL} in (13). In principle, the iterative bi-directional training comprising the above signaling can be integrated into the flexible 5G 3GPP NR frame/slot structure, as discussed in [20], [21]. Table I shows the minimum number of orthogonal pilots (and thus the minimum number of pilot symbols) necessary for the iterative bi-directional training in the proposed distributed precoding designs and in the reference precoding schemes illustrated in Section III-C.

Remark 5. The *Distributed GB*, if implemented via backhaul signaling for the CSI exchange similarly to [19], would still require the UE-specific effective uplink channel estimation (see Section II-A) and would generate the same backhaul signaling overhead as the *Distributed BR* described in Section IV-A. In fact, reconstructing the cross terms $\xi_{b,g}$ in (40) at BS b is not possible with group-specific CSI exchange. On the other hand, adopting iterative bi-directional training with the new group-specific OTA uplink training resource allows to implement the *Distributed GB* (and the *Distributed BR-GS*) with reduced overhead with respect to the *Distributed BR*.

VI. NUMERICAL RESULTS AND DISCUSSION

In this section, we compare the performance of the proposed multi-group multicast precoding designs presented in Section V, i.e., the *Distributed BR* (Algorithm 2), the *Distributed BR-GS* (Algorithm 3), and the *Distributed GB* (Algorithm 4), with that of the reference precoding schemes described in Section III-C, i.e., the *Centralized* (Algorithm 1), the *Local MMSE*, and the *Local MF*. Unless otherwise stated, the simulation setup comprises the following parameters. $B = 25$ BSs, each equipped with $M = 8$ antennas, are placed on a square grid with a distance of 100 m between neighboring BSs. $K = 32$ UEs, each equipped with $N = 2$ antennas, are uniformly distributed across the square grid. The UEs are divided into $G = 8$ multicast groups,

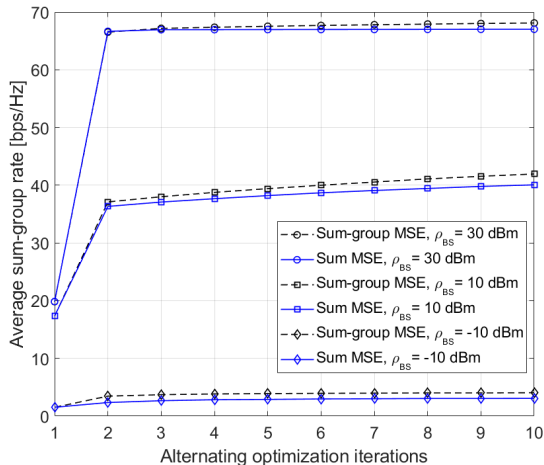


Figure 1: Average sum-group rate resulting from the sum-group MSE minimization and the sum MSE minimization versus the number of alternating optimization iterations for different values of ρ_{BS} .

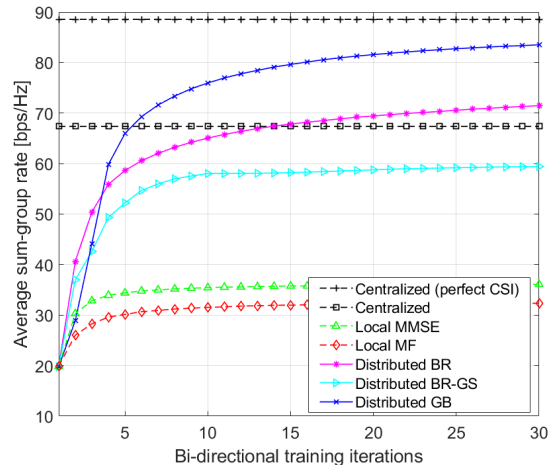


Figure 2: Average sum-group rate versus the number of bi-directional training iterations.

each consisting of 4 randomly selected UEs. Assuming uncorrelated Rayleigh fading, the entries of $\mathbf{H}_{b,k}$ are i.i.d. $\mathcal{CN}(0, \delta_{b,k})$ random variables, where $\delta_{b,k} \triangleq -48 - 30 \log_{10}(d_{b,k})$ [dB] is the large-scale fading coefficient and $d_{b,k}$ is the distance between BS b and UE k .² The maximum transmit power for both data and the pilot transmission is $\rho_{BS} = 30$ dBm at the BSs and $\rho_{UE} = 20$ dBm at the UEs. The AWGN power at the BSs and at the UEs is fixed to $\sigma_{BS}^2 = \sigma_{UE}^2 = -95$ dBm. As a performance metric, we evaluate the sum-group rate in (3) averaged over 10^3 independent channel realizations and UE drops. In all the algorithms, the combiners at the UEs are initialized with random vectors and the step sizes are appropriately chosen to promote an aggressive reduction of the sum MSE objective during the first few iterations.

We begin by validating Proposition 1 considering a centralized implementation. Figure 1 compares the average sum-group rate resulting from the sum-group MSE minimization (see Section III-A) and the sum MSE minimization (see Section III-B) for different values of ρ_{BS} . We observe that, as the SNR increases, the gap between the two curves does not increase. Therefore, at high SNR, the sum-group rate obtained with the sum MSE minimization closely approximates the one resulting from the sum-group MSE minimization.

Figure 2 illustrates the average sum-group rate versus the number of bi-directional training iterations, where the *Centralized* with perfect CSI is also included as an upper bound. The proposed distributed precoding designs greatly outperform the local precoding designs. During

²The simulation results would be very similar with correlated channel models such as the one-ring model [33].

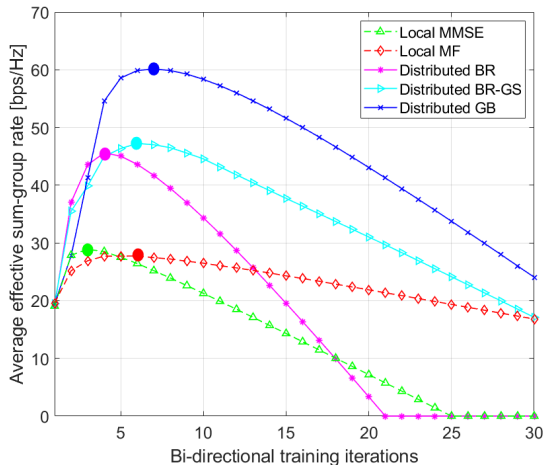


Figure 3: Average effective sum-group rate versus the number of bi-directional training iterations, with $r_t = 1000$.

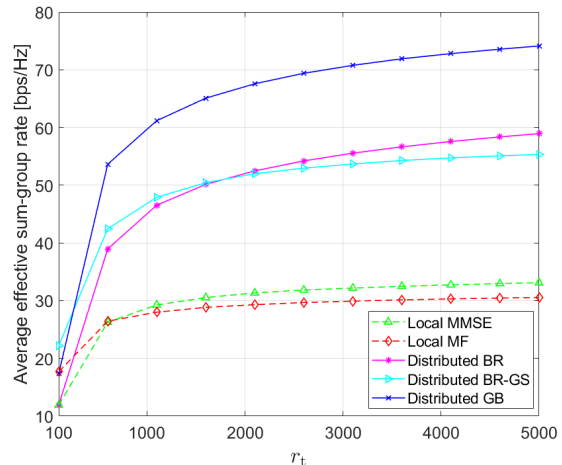


Figure 4: Average effective sum-group rate versus the resource block size.

the first few iterations, the *Distributed BR* and the *Distributed BR-GS* are superior to the *Distributed GB*. Indeed, in the distributed precoding designs with best-response updates, each BS greedily aims to reduce its individual MSE by exploiting its local interference covariance matrix, leading to a slower convergence to a solution of the sum MSE minimization. On the other hand, the *Distributed GB* directly targets to reduce the sum MSE and thus outperforms all the other distributed algorithms after a few iterations. The proposed distributed precoding designs eventually provide a better sum-group rate than the *Centralized*. In fact, the iterative bi-directional training involves multiple pilot-aided channel estimations with independent AWGN realizations, whereas only one (antenna-specific) noisy channel estimate is used in the *Centralized* (see [20]). As expected, the *Local MMSE* is the best among the local precoding designs as it exploits the local interference covariance matrix that is not considered in the *Local MF*.

In the following, we compare the effective performance of the distributed precoding designs in terms of the effective sum-group rate, defined as

$$R_{\text{eff}}^{(i)} \triangleq \left(1 - i \frac{r_{\text{ce}}}{r_t}\right) R^{(i)}, \quad (63)$$

where r_{ce} is the number of pilot symbols used in each bi-directional training iteration and r_t is the size of the resource block including the transmission of both the data symbols and the pilot symbols. The switching time between downlink and uplink training instances is neglected. Figure 3 plots the average effective sum-group rate versus the number of bi-directional training iterations given a resource block size $r_t = 1000$. All the implementations achieve the maximum (indicated by larger

dots) effective sum-group rate within a few iterations. After the maximum point, the performance starts to decrease as the number of available data symbols for communication is reduced linearly with each bi-directional training iteration. As shown in Table I, the *Distributed BR-GS* uses fewer pilot symbols than the *Distributed BR*. As a result, the effective sum-group rate of the *Distributed BR-GS* is slightly better than the *Distributed BR*, even though without the training overhead, the sum-group rate of the *Distributed BR-GS* is inferior to the *Distributed BR* (as shown in Figure 2). Similarly, the performance of the *Local MF* is close to the *Local MMSE* because fewer pilot symbols are required per iteration. The effective sum-group rate of the *Distributed GB* is superior to all the other methods. Furthermore, the training overhead is smaller than for the *Distributed BR* approach due to the use of group-specific pilots. In this example, at the maximum point, the *Distributed BR*, the *Distributed BR-GS*, and the *Distributed GB* provide 1.6, 1.65, and 2.1 times higher effective sum-group rate than the *Local MMSE* and the *Local MF*, respectively.

In Figure 4, the effective sum-group rate is depicted with respect to the resource block size r_t . For example, for $r_t = 1000$, the effective sum-group rate of all the methods shown in Figure 4 corresponds to their respective maximum value of the effective sum-group rates in Figure 3. Note that the optimal number of bi-directional training iterations to obtain the maximum effective sum-group rate increases with r_t as a higher training overhead can be tolerated. In general, distributed bi-directional training methods perform well for resource block sizes $r_t \geq 500$. For example, with $r_t = 500$, the *Distributed GB* greatly outperforms all the other methods. However, the *Distributed BR-GS* performs better than the *Distributed BR* due to the use of fewer pilot symbols in each bi-directional training iteration and despite the extra interference term in (60). With large resource blocks, the training overhead becomes insignificant, and the performance approaches to Figure 2, which do not account for the training overhead.

Figure 5 plots the effective sum-group rate versus the number of UEs in each group $|\mathcal{K}_g|$ for $r_t = 1000$. The sum-group rates are decreased when $|\mathcal{K}_g|$ is increased as more spatial degrees of freedom are used to suppress the interference across the multicast groups. However, at the same time, the sum rate across all the UEs $\sum_{g \in \mathcal{G}} |\mathcal{K}_g| R_g$ is increased. The training overhead associated with $\mathbf{X}_k^{\text{UL-1}}$ in the *Distributed BR* and the *Local MMSE* depends on $K = \sum_{g \in \mathcal{G}} |\mathcal{K}_g|$, while the training overhead associated with $\mathbf{X}_k^{\text{UL-2}}$ for the *Distributed BR-GS*, the *Distributed GB*, and the *Local MF* is dictated by G . Consequently, the *Distributed BR* and the *Local MMSE* are more severely penalized by an increase in K . For example, considering the case of $|\mathcal{K}_g| = 16$, the performance of the *Distributed BR* and the *Local MMSE* is inferior even to that of the *Local MF*.

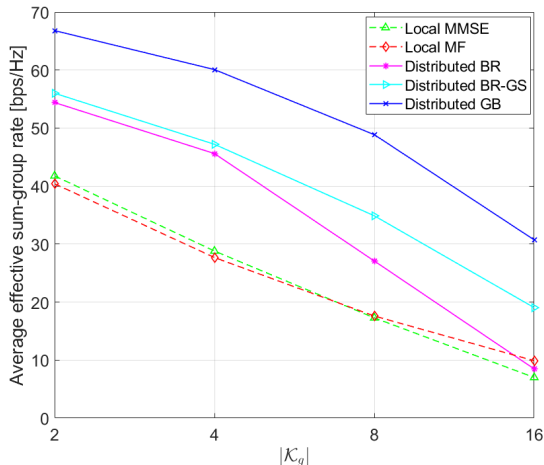


Figure 5: Average effective sum-group rate versus the number of UEs in each group, with $r_t = 1000$.

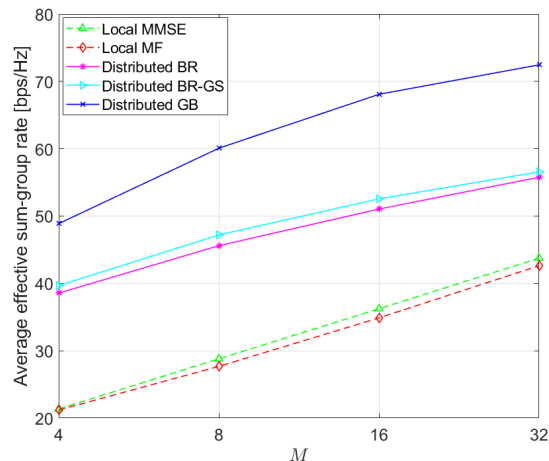


Figure 6: Average effective sum-group rate versus the number of antennas at each BS, with $r_t = 1000$.

Figure 6 depicts the effective sum-group rate as a function of M for $r_t = 1000$. Increasing M obviously improves the performance of all the considered methods. What is more, the proposed distributed precoding designs provide significant gains over the local precoding designs even with a relatively high number of BS antennas, e.g., $M = 32$, which motivates the use of distributed precoding design even in such scenarios.

The performance of the proposed distributed precoding designs at low SNR, where the joint interference suppression across the BSs becomes less important, is captured in Figure 7. Still, the *Distributed GB* is superior to all the other methods, whereas the *Distributed BR-GS*, which depends now on the noisy feedback with the extra interference term in (60), suffers from inaccuracies in the local interference covariance matrix, making it inferior to the local precoding methods.

In Figure 8, the performance of the proposed multicast precoding designs is compared with the corresponding unicast precoding design for 32 UEs with 8 groups and 4 UEs in each group. For the case of unicasting, we assume that the same data (with distinctly modulated symbols among the UEs) is to be delivered to all the UEs in a given group using UE-specific precoders. Since the same data needs to be delivered to all $|\mathcal{K}_g|$ users within a given time, the rate is bounded by the worst UE in the group, similar to the multicasting scenario. Hence, we use similar rate calculations as in (3) to evaluate the unicasting performance but with the UE-specific precoder designed to minimize the sum-MSE objective as in [20]. The precoding design for unicasting requires UE-specific pilots, which increases the CSI estimation accuracy. To show a fair comparison between the multicasting and the unicasting designs, the transmission power of the

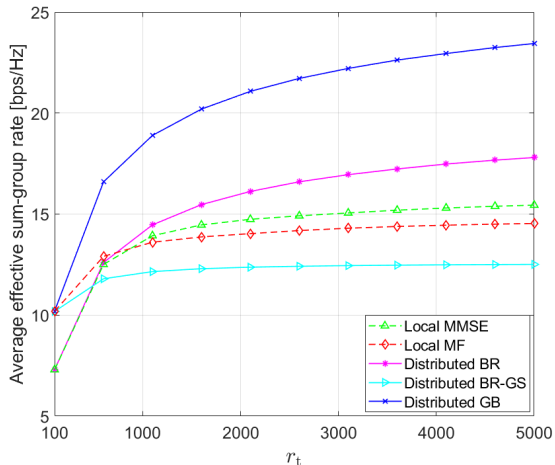


Figure 7: Average effective sum-group rate versus the resource block size at low SNR ($\sigma_{\text{BS}}^2 = \sigma_{\text{UE}}^2 = -75$ dBm).

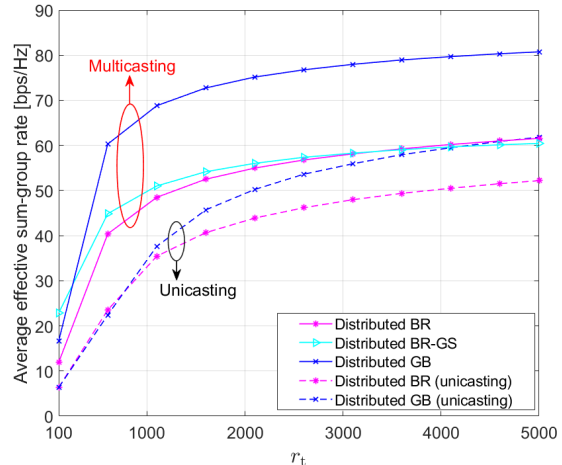


Figure 8: Average effective sum-group rate versus the resource block size in comparison with the unicast scenario [20] with the same CSI accuracy.

group-specific pilots in multicasting is scaled accordingly to have similar CSI estimation accuracy for both cases. The results in Figure 8 demonstrate that the performance of unicast is inferior to multicasting for all the proposed precoding design methods. In general, unicast beamforming needs to suppress interference towards all other UEs while only the other group UEs need to be considered for multicast design. Moreover, unicast requires more resources for training, which increases the training overhead for small r_t . For $r_t = 1000$, for example, the unicast based on the *Distributed GB* design (considering single UE as a group in Section V-C) delivers ~ 4.5 bps/Hz per UE, whereas the corresponding multicast design provides ~ 8.5 bps/Hz. Finally, comparing the unicast results from Figure 8 to the multicasting results with uncompensated pilot powers in Figure 4, it is evident that the multicasting schemes based on group-specific pilots still greatly outperform the unicast schemes with UE-specific pilots.

VII. CONCLUSIONS

Distributed multi-group multicast precoding designs are proposed for cell-free massive MIMO systems relying on minimal OTA training overhead. The sum-group MSE minimization is initially considered to guarantee absolute MSE fairness within each multicast group. Subsequently, to simplify the computation and signaling, the sum-group MSE is approximated with the sum MSE objective. Considering the UE-specific rates as the performance metric, the aforementioned approximation holds well, especially at high SNR. An iterative bi-directional training is adopted to design the precoders and the combiners locally at each BS and at each UE, respectively.

To this end, a new group-specific OTA uplink training resource is introduced to obtain the required group-specific cross terms from other BSs in the distributed precoding design, which eliminates the need for backhaul signaling to exchange the CSI. Furthermore, the distributed precoding designs are implemented by means of either the best-response or gradient-based updates exploiting the UE-specific and (or) group-specific pilots. Consequently, the distributed precoding designs with the best-response updates result in a steepest descent direction for the sum MSE minimization, which is inferior to its centralized design. However, the gradient-based update solves the sum MSE minimization as it is in a centralized design. Numerical results show that the distributed gradient-based precoding methods with group-specific pilots always yield the best effective performance. Moreover, all the proposed distributed precoding designs greatly outperform conventional cell-free massive MIMO precoding designs that rely solely on local CSI.

APPENDIX I

SUB-GRADIENT UPDATE OF $\{\mu_k\}_{k \in \mathcal{K}}$ AND $\{\lambda_b\}_{b \in \mathcal{B}}$

1) *Sub-gradient update of $\{\mu_k\}_{k \in \mathcal{K}}$.* The optimality condition for t_g is given by

$$\frac{\partial}{\partial t_g} \mathcal{L}_{(22)}(\{\mathbf{w}_g, t_g, \mu_k, \lambda_b\}) = 0 \implies \sum_{k \in \mathcal{K}_g} \mu_k = 1. \quad (64)$$

Moreover, the complementary slackness conditions corresponding to the per-UE MSE constraint in (18) are given by

$$\mu_k(\text{MSE}_k - t_g) = 0, \quad \forall k \in \mathcal{K}_g, \implies \sum_{k \in \mathcal{K}_g} \mu_k t_g = \sum_{k \in \mathcal{K}_g} \mu_k \text{MSE}_k. \quad (65)$$

Therefore, from (64) and (65), we have $t_g = \sum_{k \in \mathcal{K}_g} \mu_k \text{MSE}_k$. To achieve absolute MSE fairness within each multicast group, each μ_k is updated as [6]

$$\mu_k^{(i)} = \max \left(0, \mu_k^{(i-1)} + \zeta \frac{\partial}{\partial \mu_k} \mathcal{L}_{(22)}(\{\mathbf{w}_g, t_g, \mu_k, \lambda_b\}) \right) = \max \left(0, \mu_k^{(i-1)} + \zeta (\text{MSE}_k - t_g) \right), \quad (66)$$

where i is the iteration index and ζ is the step size. Finally, (66) is normalized to meet the constraint in (64).

2) *Sub-gradient update of $\{\lambda_b\}_{b \in \mathcal{B}}$.* To meet the per-BS transmit power constraint, λ_b is updated as [29]

$$\lambda_b^{(i)} = \max \left(0, \lambda_b^{(i-1)} + \eta \frac{\partial}{\partial \lambda_b} \mathcal{L}_{(22)}(\{\mathbf{w}_g, t_g, \mu_k, \lambda_b\}) \right) = \max \left(0, \lambda_b^{(i-1)} + \eta \left(\sum_{g \in \mathcal{G}} \|\mathbf{w}_{b,g}\|^2 - \rho_{\text{BS}} \right) \right), \quad (67)$$

where η is the step size.

APPENDIX II
KKT CONDITIONS OF (29)

The Lagrangian of (29) can be written as

$$\mathcal{L}_{(29)}(\{p_g, \kappa\}) \triangleq \sum_{k \in \mathcal{K}} \frac{\sigma_{\text{UE}}^2}{p_{gk} c_{kk}^2} + \kappa \left(\sum_{\bar{g} \in \mathcal{G}} p_{\bar{g}} - \rho_{\text{BS}} \right), \quad (68)$$

where κ is the dual variable corresponding to the constraint in (29). Then, the optimal p_g is obtained as

$$\frac{\partial}{\partial p_g} \mathcal{L}_{(29)}(\{p_g, \kappa\}) = 0 \implies p_g = \sqrt{\sum_{k \in \mathcal{K}_g} \frac{\sigma_{\text{UE}}^2}{\kappa c_{kk}^2}}. \quad (69)$$

Finally, κ is computed to satisfy $\sum_{g \in \mathcal{G}} p_g = \rho_{\text{BS}}$, which yields

$$\kappa = \frac{1}{\rho_{\text{BS}}^2} \left(\sum_{g \in \mathcal{G}} \sqrt{\sum_{k \in \mathcal{K}_g} \frac{\sigma_{\text{UE}}^2}{c_{kk}^2}} \right)^2. \quad (70)$$

REFERENCES

- [1] B. Gouda, I. Atzeni, and A. Tölli, "Distributed precoding design for multi-group multicasting in cell-free massive MIMO," in *Proc. IEEE Global Commun. Conf. (GLOBECOM)*, Rio de Janeiro, Brazil, Dec. 2022. [Online]. Available: <https://arxiv.org/pdf/2211.05522.pdf>
- [2] N. Rajatheva, I. Atzeni, E. Björnson *et al.*, "White paper on broadband connectivity in 6G," Jun. 2020, White Paper.
- [3] N. Sidiropoulos, T. Davidson, and Z.-Q. Luo, "Transmit beamforming for physical-layer multicasting," *IEEE Trans. Signal Process.*, vol. 54, no. 6, pp. 2239–2251, Jun. 2006.
- [4] E. Karipidis, N. D. Sidiropoulos, and Z.-Q. Luo, "Quality of service and max-min fair transmit beamforming to multiple cochannel multicast groups," *IEEE Trans. Signal Process.*, vol. 56, no. 3, pp. 1268–1279, Mar. 2008.
- [5] M. Dong and Q. Wang, "Multi-group multicast beamforming: Optimal structure and efficient algorithms," *IEEE Trans. Signal Process.*, vol. 68, pp. 3738–3753, May 2020.
- [6] H. B. Mahmoodi, B. Gouda, M. Salehi, and A. Tölli, "Low-complexity multicast beamforming for multi-stream multi-group communications," in *Proc. IEEE Global Commun. Conf. (GLOBECOM)*, Madrid, Spain, Dec. 2021.
- [7] H. Yang, T. L. Marzetta, and A. Ashikhmin, "Multicast performance of large-scale antenna systems," in *Proc. IEEE Int. Workshop Signal Process. Adv. in Wireless Commun. (SPAWC)*, Darmstadt, Germany, Jun. 2013.
- [8] M. Sadeghi, E. Björnson, E. G. Larsson, C. Yuen, and T. L. Marzetta, "Max-min fair transmit precoding for multi-group multicasting in massive MIMO," *IEEE Trans. Wireless Commun.*, vol. 17, no. 2, pp. 1358–1373, Feb. 2018.
- [9] M. Sadeghi, E. Björnson, E. G. Larsson, C. Yuen, and T. Marzetta, "Joint unicast and multi-group multicast transmission in massive MIMO systems," *IEEE Trans. Wireless Commun.*, vol. 17, no. 10, pp. 6375–6388, Jul. 2018.
- [10] Z. Xiang, M. Tao, and X. Wang, "Coordinated multicast beamforming in multicell networks," *IEEE Trans. Wireless Commun.*, vol. 12, no. 1, pp. 12–21, Jan. 2013.
- [11] P. Song, G. Scutari, F. Facchinei, and L. Lampariello, "D3M: Distributed multi-cell multigroup multicasting," in *Proc. IEEE Int. Conf. Acoust., Speech, and Signal Process. (ICASSP)*, Shanghai, China, Mar. 2016.
- [12] O. Tervo, H. Pennanen, S. Chatzinotas, B. Ottersten, and M. Juntti, "Multi-cell interference coordination for multigroup multicast transmission," in *Proc. Int. European Conf. on Netw. and Commun. (EuCNC)*, Oulu, Finland, Jun. 2017.

- [13] H. Q. Ngo, A. Ashikhmin, H. Yang, E. G. Larsson, and T. L. Marzetta, “Cell-free massive MIMO versus small cells,” *IEEE Trans. Wireless Commun.*, vol. 16, no. 3, pp. 1834–1850, Mar. 2017.
- [14] E. Björnson and L. Sanguinetti, “Scalable cell-free massive MIMO systems,” *IEEE Trans. Commun.*, vol. 68, no. 7, pp. 4247–4261, Jul. 2020.
- [15] G. Interdonato, M. Karlsson, E. Björnson, and E. G. Larsson, “Local partial zero-forcing precoding for cell-free massive MIMO,” *IEEE Trans. Wireless Commun.*, vol. 19, no. 7, pp. 4758–4774, Jul. 2020.
- [16] E. Björnson and L. Sanguinetti, “Making cell-free massive MIMO competitive with MMSE processing and centralized implementation,” *IEEE Trans. Wireless Commun.*, vol. 19, no. 1, pp. 77–90, Jan. 2020.
- [17] L. Du, L. Li, H. Q. Ngo, T. C. Mai, and M. Matthaiou, “Cell-free massive MIMO: Joint maximum-ratio and zero-forcing precoder with power control,” *IEEE Trans. Commun.*, vol. 69, no. 6, pp. 3741–3756, Jun. 2021.
- [18] L. Miretti, E. Björnson, and D. Gesbert, “Team MMSE precoding with applications to cell-free massive MIMO,” *IEEE Trans. Wireless Commun.*, 2022.
- [19] J. Kaleva, A. Tölli, M. Juntti, R. A. Berry, and M. L. Honig, “Decentralized joint precoding with pilot-aided beamformer estimation,” *IEEE Trans. Signal Process.*, vol. 66, no. 9, pp. 2330–2341, May 2018.
- [20] I. Atzeni, B. Gouda, and A. Tölli, “Distributed precoding design via over-the-air signaling for cell-free massive MIMO,” *IEEE Trans. Wireless Commun.*, vol. 20, no. 2, pp. 1201–1216, Feb. 2021.
- [21] A. Tölli, H. Ghach, J. Kaleva *et al.*, “Distributed coordinated transmission with forward-backward training for 5G radio access,” *IEEE Commun. Mag.*, vol. 57, no. 1, pp. 58–64, Jan. 2019.
- [22] T. X. Doan, H. Q. Ngo, T. Q. Duong, and K. Tourki, “On the performance of multigroup multicast cell-free massive MIMO,” *IEEE Commun. Lett.*, vol. 21, no. 12, pp. 2642–2645, Dec. 2017.
- [23] Y. Zhang, H. Cao, and L. Yang, “Max-min power optimization in multigroup multicast cell-free massive MIMO,” in *Proc. IEEE Wireless Commun. and Netw. Conf. (WCNC)*, Marrakech, Morocco, Oct. 2019.
- [24] M. Farooq, M. Juntti, and L.-N. Tran, “Power control for multigroup multicast cell-free massive MIMO downlink,” in *Proc. European Signal Process. Conf. (EUSIPCO)*, Dublin, Ireland, Dec. 2021.
- [25] I. Atzeni, B. Gouda, and A. Tölli, “Distributed joint receiver design for uplink cell-free massive MIMO,” in *Proc. IEEE Int. Conf. Commun. (ICC)*, Dublin, Ireland, Jun. 2020.
- [26] G. Caire, “On the ergodic rate lower bounds with applications to massive MIMO,” *IEEE Trans. Wireless Commun.*, vol. 17, no. 5, pp. 3258–3268, May 2018.
- [27] P. Jayasinghe, A. Tölli, J. Kaleva, and M. Latva-aho, “Bi-directional beamformer training for dynamic TDD networks,” *IEEE Trans. Signal Process.*, vol. 66, no. 23, pp. 6252–6267, Dec. 2018.
- [28] M. Grant and S. Boyd, “CVX: Matlab software for disciplined convex programming, version 2.1,” Mar. 2014.
- [29] P. Komulainen, A. Tölli, and M. Juntti, “Effective CSI signaling and decentralized beam coordination in TDD multi-cell MIMO systems,” *IEEE Trans. Signal Process.*, vol. 61, no. 9, pp. 2204–2218, May 2013.
- [30] S. Chen, J. Zhang, J. Zhang, E. Björnson, and B. Ai, “A survey on user-centric cell-free massive MIMO systems,” *Digital Commun. and Netw.*, Dec. 2021.
- [31] G. Scutari, F. Facchinei, P. Song, D. P. Palomar, and J.-S. Pang, “Decomposition by partial linearization: Parallel optimization of multi-agent systems,” *IEEE Trans. Signal Process.*, vol. 62, no. 3, pp. 641–656, Feb. 2014.
- [32] S. Boyd and L. Vandenberghe, *Convex optimization*. Cambridge University Press, 2004.
- [33] A. Abdi and M. Kaveh, “A space-time correlation model for multielement antenna systems in mobile fading channels,” *IEEE J. Sel. Areas Commun.*, vol. 20, no. 3, pp. 550–560, Apr. 2002.